

UC Santa Cruz

UC Santa Cruz Previously Published Works

Title

Search for the decay $B_s^0 \rightarrow \mu^+ \mu^-$ with the ATLAS detector

Permalink

<https://escholarship.org/uc/item/77x05006>

Journal

Physics Letters, Section B: Nuclear, Elementary Particle and High-Energy Physics, 713(4-5)

ISSN

0370-2693

Authors

Aad, G
Abbott, B
Abdallah, J
[et al.](#)

Publication Date

2012-07-18

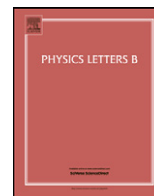
DOI

10.1016/j.physletb.2012.06.013

Copyright Information

This work is made available under the terms of a Creative Commons Attribution License, available at <https://creativecommons.org/licenses/by/4.0/>

Peer reviewed



Search for the decay $B_s^0 \rightarrow \mu^+ \mu^-$ with the ATLAS detector[☆]

ATLAS Collaboration^{*}

ARTICLE INFO

Article history:

Received 4 April 2012

Received in revised form 2 June 2012

Accepted 6 June 2012

Available online 12 June 2012

Editor: H. Weerts

Keywords:

B meson

Rare decays

FCNC

ATLAS

LHC

ABSTRACT

A blind analysis searching for the decay $B_s^0 \rightarrow \mu^+ \mu^-$ has been performed using proton–proton collisions at a centre-of-mass energy of 7 TeV recorded with the ATLAS detector at the LHC. With an integrated luminosity of 2.4 fb^{-1} no excess of events over the background expectation is found and an upper limit is set on the branching fraction $\text{BR}(B_s^0 \rightarrow \mu^+ \mu^-) < 2.2(1.9) \times 10^{-8}$ at 95% (90%) confidence level.

© 2012 CERN. Published by Elsevier B.V. Open access under [CC BY-NC-ND license](#).

1. Introduction

Flavour changing neutral current processes are highly suppressed in the Standard Model (SM), and therefore their study is of particular interest in the search for new physics. The SM predicts the branching fraction for the decay $B_s^0 \rightarrow \mu^+ \mu^-$ to be extremely small: $(3.5 \pm 0.3) \times 10^{-9}$ [1–4]. This process might be substantially enhanced by coupling to non-SM heavy particles, such as those predicted by the Minimal Supersymmetric Standard Model [5–11] and other extensions [12]. Upper limits on this branching fraction, in the range $(0.45\text{--}5.1) \times 10^{-8}$, have been reported by the D0 [13], CDF [14], CMS [15,16] and LHCb [17,18] Collaborations. This Letter reports the result of a search performed with pp collisions corresponding to an integrated luminosity of 2.4 fb^{-1} , collected in the first half of the 2011 data-taking period using the ATLAS detector at the LHC.

The analysis is based on events selected with a di-muon trigger and reconstructed in the ATLAS inner tracking detector and muon spectrometer [19]. Details of the detector, trigger and datasets are discussed in Section 2, together with the preselection criteria.

The $B_s^0 \rightarrow \mu^+ \mu^-$ branching fraction is measured with respect to a prominent reference decay ($B^\pm \rightarrow J/\psi K^\pm$) in order to minimize systematic uncertainties in the evaluation of the efficiencies and acceptances, while still providing small statistical uncertainties. The branching fraction can be written as

$$\text{BR}(B_s^0 \rightarrow \mu^+ \mu^-) = \text{BR}(B^\pm \rightarrow J/\psi K^\pm \rightarrow \mu^+ \mu^- K^\pm) \times \frac{f_u}{f_s} \times \frac{N_{\mu^+ \mu^-}}{N_{J/\psi K^\pm}} \times \frac{A_{J/\psi K^\pm}}{A_{\mu^+ \mu^-}} \frac{\epsilon_{J/\psi K^\pm}}{\epsilon_{\mu^+ \mu^-}}, \quad (1)$$

where the right-hand side includes the $B^\pm \rightarrow J/\psi K^\pm \rightarrow \mu^+ \mu^- K^\pm$ branching fraction, the relative production probability of B^\pm and B_s^0 f_u/f_s taken from previous measurements [20–22], the event yields after background subtraction, and the acceptance and efficiency ratios. The event yields for both signal and reference channels were obtained from signal and sideband (background) regions defined in the invariant-mass spectrum (see Table 1).

The Single Event Sensitivity (SES) corresponds to the $B_s^0 \rightarrow \mu^+ \mu^-$ branching fraction which would yield one observed signal event in the data sample:

$$\text{BR}(B_s^0 \rightarrow \mu^+ \mu^-) = N_{\mu^+ \mu^-} \times \text{SES}, \quad (2)$$

where $N_{\mu^+ \mu^-}$ is the number of observed events.

This Letter describes the results of a blind analysis in which the di-muon mass region 5066 to 5666 MeV was removed from the analysis until the procedures for event selection, signal and limit extractions were fully defined. Sections 3.1 to 3.3 discuss the variables used in the event selection, Monte Carlo (MC) tuning and background studies. The final sample of candidates was selected with a multivariate classifier, trained on a fraction of the events from the di-muon invariant-mass sidebands, as discussed in Section 3.4. The relative efficiency and event yields in the reference channel are discussed in Sections 4.1 and 4.2, respectively. The signal extraction is discussed in Section 5 and the corresponding limit on the branching fraction is presented in Section 6.

[☆] © CERN for the benefit of the ATLAS Collaboration.

^{*} E-mail address: atlas.publications@cern.ch.

According to the SM, the branching fraction $\text{BR}(B^0 \rightarrow \mu^+\mu^-)$ is predicted to be about 30 times smaller than $\text{BR}(B_s^0 \rightarrow \mu^+\mu^-)$ [1,2]. Therefore, despite the increased SES of approximately a factor four due to the absence of the factor f_u/f_s and possible enhancements due to new physics, the sensitivity to this channel is beyond the reach of the current analysis. Hence only a limit on $\text{BR}(B_s^0 \rightarrow \mu^+\mu^-)$ was derived by assuming $\text{BR}(B^0 \rightarrow \mu^+\mu^-)$ to be negligible.

2. ATLAS detector, data and simulation samples

The ATLAS detector¹ consists of three main components: an Inner Detector tracking system (ID) immersed in a 2 T magnetic field, a system of electromagnetic and hadronic calorimeters, and an outer Muon Spectrometer (MS). A full description can be found in [19]. The detector performance characteristics most relevant to this analysis are the vertex-finding and the overall track reconstruction in the ID and MS, together with the ability of the trigger system to record events containing pairs of muons.

The ID provides precise track reconstruction within the pseudorapidity range $|\eta| < 2.5$. It employs a Pixel detector close to the beam pipe, a silicon microstrip detector (SCT) at intermediate radii and a Transition Radiation Tracker (TRT) at outer radii. The innermost Pixel layer is located at a radius of 50.5 mm and plays a key role in precise vertex determination.

The MS comprises separate trigger and high-precision tracking chambers that measure the deflection of muons in a toroidal magnetic field. The precision chambers cover the region $|\eta| < 2.7$ and measure the coordinate in the bending plane. The trigger chambers cover the range $|\eta| < 2.4$ and provide fast coarser measurements in both the bending and non-bending plane.

This analysis is based on a sample of pp collisions at $\sqrt{s} = 7$ TeV, recorded by ATLAS in the period April–August 2011. Trigger and pile-up conditions changed for data taken after this period: the remainder of the 2011 dataset will be included in a future analysis. Data used in the analysis were recorded during stable LHC beam periods. Further data quality requirements were also imposed, notably on the performance of the MS and ID systems. The total integrated luminosity amounts to 2.4 fb^{-1} . This sample has an average of about five primary vertices per event from multiple proton–proton interactions.

A muon trigger [23] was used to select events. In particular, the sample contains events seeded by a Level-1 di-muon trigger which required a transverse momentum $p_T > 4$ GeV for both muon candidates. A full track reconstruction of the muon candidates was performed at the second and third trigger levels, where additional cuts on the di-muon invariant mass $m_{\mu^+\mu^-}$ were applied, loosely selecting events compatible with J/ψ (2500 to 4300 MeV) or B_s^0 (4000 to 8500 MeV) decays into a muon pair.

Events containing candidates for $B_s^0 \rightarrow \mu^+\mu^-$, $B^\pm \rightarrow J/\psi K^\pm \rightarrow \mu^+\mu^- K^\pm$ and, as discussed in Sections 3.2 and 3.3, $B_s^0 \rightarrow J/\psi \phi \rightarrow \mu^+\mu^- K^+K^-$ were retained for this analysis. After cutting on the mass of the intermediate resonances ($1009 \text{ MeV} \leq m_\phi \leq 1031 \text{ MeV}$, $2915 \text{ MeV} \leq m_{J/\psi} \leq 3175 \text{ MeV}$) a preselection was applied, based on track properties and the quality of the reconstructed B decay vertex. All charged particle tracks reconstructed in the ID were required to have at least one Pixel, six SCT and eight TRT hits. Tracks were required to have $|\eta| < 2.5$ and

Table 1

Definition of the signal and sideband regions used in this analysis.

Channel	Signal region	Sideband regions
$B_s^0 \rightarrow \mu^+\mu^-$	[5066, 5666] MeV	[4766, 5066] MeV [5666, 5966] MeV
$B^\pm \rightarrow J/\psi K^\pm$	[5180, 5380] MeV	[4930, 5130] MeV [5430, 5630] MeV

$p_T > 4$ GeV (> 2.5 GeV) for muon (kaon) candidates. No particle identification was used to distinguish K^\pm and π^\pm candidates. ID tracks that were matched to reconstructed MS tracks were selected as candidate muons. Decay vertices were formed by combining two, three or four tracks, according to the specific decay process [24]. All B -meson properties were computed based on the result of the fit of the tracks to the B decay vertex. In order to reject fake track combinations, the fit χ^2 per degree of freedom was required to be less than 2.0 (85% efficient) for $B_s^0 \rightarrow \mu^+\mu^-$ and less than 6.0 (99.5% efficient) for the other channels. All reconstructed B candidates were required to satisfy $p_T^B > 8.0$ GeV and $|\eta^B| < 2.5$ in order to define our efficiencies and acceptances within a fiducial phase-space volume with as little as possible reliance on MC extrapolations. Signal and sideband regions were defined according to Table 1.

The primary vertex position was obtained from a fit of charged tracks not used in the decay vertex and constrained to the interaction region of the colliding beams. If multiple candidate primary vertices were present, the one closest in z to the decay vertex was chosen. After preselection, approximately 2×10^5 $B_s^0 \rightarrow \mu^+\mu^-$ and 1.4×10^5 $B^\pm \rightarrow J/\psi K^\pm$ candidates were obtained in the signal regions.

Samples of Monte Carlo (MC) events were used for the extraction of acceptance and efficiency ratios. MC samples were produced for the signal channel $B_s^0 \rightarrow \mu^+\mu^-$, the reference channel $B^\pm \rightarrow J/\psi K^\pm$ ($J/\psi \rightarrow \mu^+\mu^-$) and the control channel $B_s^0 \rightarrow J/\psi \phi$ ($\phi \rightarrow K^+K^-$). These samples were generated with PYTHIA 6.4 [25] using the 2010 ATLAS [24,26] tune. MC events were filtered before detector simulation to ensure the presence of at least one decay of interest, with B decay products all satisfying $|\eta| < 2.5$ and $p_T > 2.5(0.5)$ GeV for muons (kaons). An additional sample was generated with a fictitious value of the B_s^0 mass (6500 MeV) and the same parameters as the standard $B_s^0 \rightarrow \mu^+\mu^-$ sample, allowing a check of the full analysis on a signal-free region before unblinding. The ATLAS detector and its response were simulated using GEANT4 [27]. Additional pp interactions in the same and nearby bunch crossings (pile-up) were included in the simulation.

3. Event selection

This section describes the expected background composition, the discriminating variables used as input to the multivariate classifier, the tuning of the simulation for the determination of the signal efficiency, the data samples used to estimate the background rejection and the optimization procedure. The signal efficiency was determined from MC samples, re-weighted to account for differences between data and MC simulation of the B -meson kinematics. The rejection power was tested using a sub-sample of background events from the sidebands in the di-muon mass spectrum.

3.1. Background composition

Two categories of background were considered: a continuum with a smooth dependence on the di-muon invariant mass, and sources of resonant contributions from mis-reconstructed decays.

¹ ATLAS uses a right-handed coordinate system with its origin at the nominal interaction point. The z -axis is along the beam pipe, the x -axis points to the centre of the LHC ring and the y -axis points upward. Cylindrical coordinates (r, ϕ) are used in the transverse plane, ϕ being the azimuthal angle around the beam pipe. The pseudorapidity η is defined as $\eta = -\ln[\tan(\theta/2)]$ where θ is the polar angle.

Comparisons of data and MC have shown that the combinatorial background from $b\bar{b} \rightarrow \mu^+\mu^-X$ decays provides a reasonable description for the distributions of the discriminating variables for the events found in the sidebands. The $b\bar{b} \rightarrow \mu^+\mu^-X$ MC sample used is equivalent to about 12 pb^{-1} of integrated luminosity. Such studies support the procedure of modeling the continuum background through interpolation of the di-muon yield in the sidebands, but do not reach a sufficient statistical precision. Half of the data events in the sidebands (those with odd event numbers) were used to optimize the selection procedure. The remaining events were used for the measurement of the background and for interpolation to the signal region.

Resonant background is due to B decay candidates containing either one or two hadrons erroneously identified as muons. Misidentification may be due to punch-through of a hadron to the MS or to decays in flight where the muon carries most of the hadron momentum. In either case the hadron fakes the muon signature for the purpose of this analysis. Single-fake events are due to, e.g. $B_s^0 \rightarrow K^+\mu^- \nu$, the charged K meson being mis-identified as a muon. Double-fake events are due to two-body hadronic B decays ($B \rightarrow hh$), e.g. $B_s^0 \rightarrow K^+\pi^-$, where both hadrons are mis-identified as muons. MC studies have shown that double-fake events are the main source of resonant background after the selection criteria used in this analysis. The main contribution is from $B_s^0 \rightarrow K^+K^-$, followed by $B^0 \rightarrow \pi^+\pi^-$ and $B^0 \rightarrow K^\pm\pi^\mp$ [20,28].

The simulation determined the probability for a hadron to be misidentified as a muon to be equal to $2(4)\%$ for π^\pm (K^\pm), with a relative uncertainty of 20%, validated against control samples in data [29]. The value for charged K mesons was averaged over K^+ and K^- and was found consistent with the preliminary results of data-driven studies based on the decay $D^* \rightarrow D^0\pi \rightarrow K\pi\pi$.

The expected event yield for $B \rightarrow hh$ was obtained from an estimation of the integrated luminosity, acceptance and efficiency. This constitutes a nearly irreducible background in this analysis, due to its resemblance to the actual signal.

3.2. Discriminating variables

Table 2 describes the discriminating variables used in the multivariate classifier. The $B_s^0 \rightarrow \mu^+\mu^-$ signal is characterized by the separation between the production (primary) and decay (secondary) vertices, as well as the two-body decay topology. These variables exploit such features to discriminate against potential backgrounds: pairs of prompt charged tracks (e.g. L_{xy} , ct significance, χ_{xy}^2), as well as pairs of displaced muons originating from $b\bar{b} \rightarrow \mu^+\mu^-X$ processes (e.g. d_0^{\max} , d_0^{\min}), secondary vertices with additional particles in the final state (e.g. α_{2D} , ΔR , D_{xy}^{\min} , D_z^{\min}) and non- $b\bar{b}$ processes (e.g. $I_{0.7}$, p_T^B , p_L^{\max} , p_L^{\min}).

Fig. 1 shows how the discriminating variables are distributed for signal and background. Among the discriminating variables, isolation ($I_{0.7}$) is expected to have the largest pile-up dependence. In order to minimize this dependence, the definition of $I_{0.7}$ was restricted to only include tracks originating from the primary vertex associated with the B decay. This specification makes the selection independent of pile-up, as shown in Fig. 2, where the efficiency of the selection for $B^\pm \rightarrow J/\psi K^\pm$ is shown for events with different numbers of reconstructed primary vertices, both in sideband-subtracted data and MC.

The variable $I_{0.7}$ might also be subject to differences between B_s^0 and B^\pm in the distributions of the surrounding hadrons, e.g. with harder p_T spectra for kaons produced in association with the B_s^0 in the b -quark fragmentation. As predicted by MC, significant differences were observed between $B^\pm \rightarrow J/\psi K^\pm$ and the control channel $B_s^0 \rightarrow J/\psi\phi$ in the $I_{0.7}$ distribution from data. Within sta-

Table 2

List of the discriminating variables used in this analysis to separate $B_s^0 \rightarrow \mu^+\mu^-$ signal from backgrounds. These variables are based on properties of the decay products, of the reconstructed primary (\bar{x}_{PV}) and secondary (\bar{x}_{SV}) vertices (separated by $\Delta\bar{x} = \bar{x}_{SV} - \bar{x}_{PV}$), the B -meson momentum \vec{p}^B and the properties of additional tracks from the underlying event. Variables are listed in order of relevance as ranked by the multivariate classifier used in the final signal/background separation as discussed in Section 3.4.2.

Variable	Description
$ \alpha_{2D} $ pointing angle	Absolute value of the angle in the transverse plane between $\Delta\bar{x}$ and \vec{p}^B
ΔR	Angle $\sqrt{(\Delta\phi)^2 + (\Delta\eta)^2}$ between $\Delta\bar{x}$ and \vec{p}^B
L_{xy}	Scalar product in the transverse plane of $(\Delta\bar{x} \cdot \vec{p}^B)/ \vec{p}^B ^2$
ct significance	Proper decay length $ct = L_{xy} \times m_B/p_T^B$ divided by its uncertainty
χ_{xy}^2, χ_z^2	Vertex separation significance $\Delta\bar{x}^T \cdot (\sigma_{\Delta\bar{x}}^2)^{-1} \cdot \Delta\bar{x}$ in (x, y) and z , respectively
$I_{0.7}$ isolation	Ratio of $ \vec{p}_T^B $ to the sum of $ \vec{p}_T^i $ and the transverse momenta of all tracks with $p_T > 0.5$ GeV within a cone $\Delta R < 0.7$ from the B direction, excluding B decay products
$ d_0^{\max} , d_0^{\min} $	Absolute values of the maximum and minimum impact parameter in the transverse plane of the B decay products relative to the primary vertex
$ D_{xy}^{\min} , D_z^{\min} $	Absolute values of the minimum distance of closest approach in the xy plane (or along z) of tracks in the event to the B vertex
p_T^B	B transverse momentum
p_L^{\max}, p_L^{\min}	Maximum and minimum momentum of the two muon candidates along the B direction

tistical uncertainties, the $I_{0.7}$ distribution from the MC simulation of the control channel $B_s^0 \rightarrow J/\psi\phi$ was verified to be consistent with the corresponding sideband-subtracted signal in data.

3.3. MC re-weighting and comparison to data

Monte Carlo samples were produced for the signal, reference and control channels, with specific requirements on the B -meson decay products as described above in Section 2. In order to ensure that the data are reproduced as closely as possible, the simulation was tuned by an iterative re-weighting procedure: a generator-level (GL) re-weighting based on simulation, followed by a data-driven (DD) re-weighting.

For the GL re-weighting, additional MC samples were generated without selection on the final states and over a wider range in the b -quark kinematics: $|\eta^B| < 4$ and $p_T^B > 2.5$ GeV. These samples allowed a binned (p_T^B, η^B) map of the efficiencies of the generator-level selections to be derived for both the signal and the reference MC. The inverse of such efficiencies was then used to weight events individually, thus correcting the GL biases. These corrections were applied independently to the simulated reference and signal channel samples to correct for the biases in the relative B_s^0/B^\pm acceptance induced by the generator-level selection. Possible residual biases were found to be negligible within the fiducial region $|\eta^B| < 2.5$ and $p_T^B > 8.0$ GeV.

Residual (p_T^B, η^B) differences between data and MC were observed after GL re-weighting. These were addressed with the DD re-weighting procedure, based on the comparison of MC events to the large sample of $B^\pm \rightarrow J/\psi K^\pm$ decays in collision data. In order not to correlate the re-weighting procedure with the yield measurement, only candidates with odd event numbers in the ATLAS dataset were used in this procedure, while the remaining sample was used for the yield measurement.

DD weights were determined by an iterative method, comparing re-weighted MC events with sideband-subtracted $B^\pm \rightarrow J/\psi K^\pm$ events in data. The procedure was applied separately to the B -meson variables p_T^B and η^B due to the limited num-

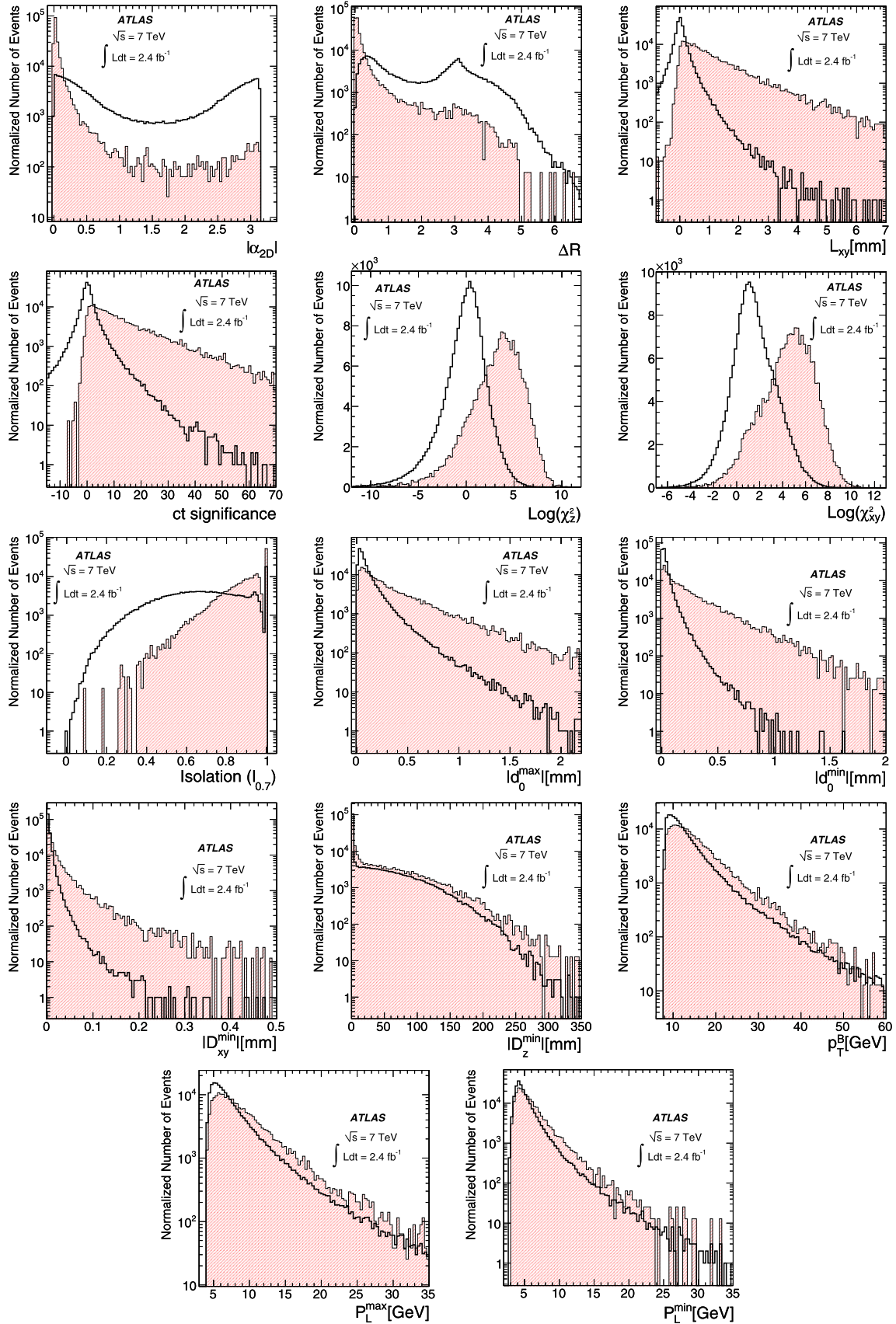


Fig. 1. Signal (filled histogram) and sideband (empty histogram) distributions for the selection variables described in Table 2. The $B_s^0 \rightarrow \mu^+ \mu^-$ signal (normalized to the background histogram) is from simulation and the background is from data in the invariant-mass sidebands.

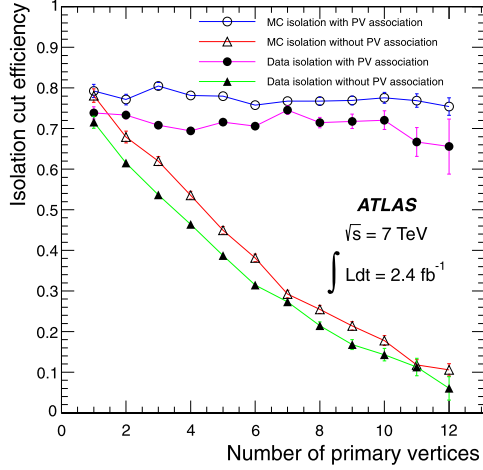


Fig. 2. Efficiency of the cut $I_{0.7} > 0.83$ as a function of the primary vertex multiplicity for $B^\pm \rightarrow J/\psi K^\pm$ candidate events from data (filled symbols) and MC simulation (empty symbols). The triangles show the efficiency when including all the tracks in the event, while circles show the same efficiency with the isolation definition used in this analysis.

ber of reconstructed $B^\pm \rightarrow J/\psi K^\pm$ events in data, deriving the weights:

$$W_{ij}(p_T^B, \eta^B) = w_i(p_T^B) \times w_j(\eta^B) \quad (3)$$

where W represents the final DD weights, the indices i and j refer to bins in p_T^B and η^B , and $w_k = N_k^{\text{data}}/N_k^{\text{MC}}$ is the data-to-MC ratio of the normalized number of entries for each variable. The convergence and the consistency of the procedure, together with the factorization assumption of Eq. (3), were tested with additional MC samples, where intentionally distorted (p_T^B, η^B) spectra were found to converge to the expected distributions. Effects related to the finite resolution in the measured variables were estimated to be smaller than 1‰ of the bin content and are therefore negligible when compared to statistical uncertainties.

Generator-level biases were addressed by applying the GL re-weighting before the DD re-weighting, and by verifying that this correction yields compatible (p_T^B, η^B) spectra for $B_s^0 \rightarrow \mu^+ \mu^-$ and $B^\pm \rightarrow J/\psi K^\pm$ MC samples. Finally, the full re-weighting procedure was applied to $B_s^0 \rightarrow J/\psi \phi$ decays, verifying within statistical uncertainty the consistency of the weights with those from $B^\pm \rightarrow J/\psi K^\pm$.

Distributions from $B^\pm \rightarrow J/\psi K^\pm$ in MC simulation and data were compared, after sideband-background subtraction, for all discriminating variables listed in Table 2 and for variables used in the preselection. Agreement between MC and data was found for most of the variables. Fig. 3 shows comparisons for L_{xy} and $I_{0.7}$. Systematic effects associated with the residual data–MC differences are discussed in Section 4. The uncertainties on the GL \times DD weights are dominated by systematic uncertainties obtained from the comparison between data and MC. They were propagated through the analysis and included among the systematic uncertainties in the signal extraction, as discussed in Section 5.

3.4. Selection optimization

The optimization of the event selection was performed by maximizing the estimator:

$$\mathcal{P} = \frac{\epsilon_{\text{sig}}}{\frac{a}{2} + \sqrt{N_{\text{bkg}}}}, \quad (4)$$

where $\epsilon_{\text{sig}} = \mathcal{A}_{\mu^+\mu^-} - \epsilon_{\mu^+\mu^-}$ and N_{bkg} are the signal acceptance times efficiency relative to the simulated phase space of the sam-

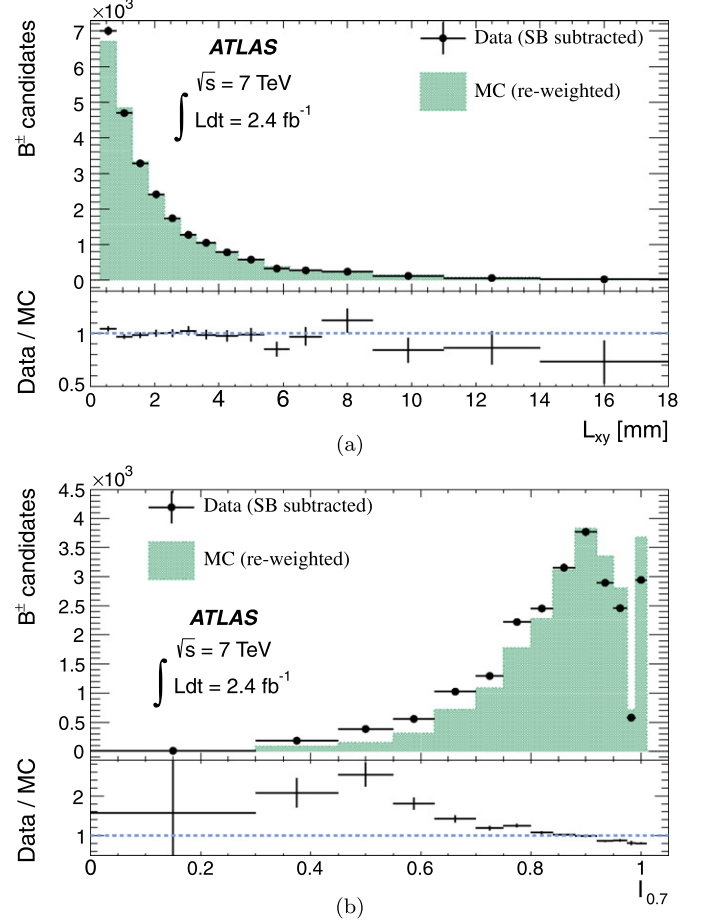


Fig. 3. Examples of sideband-subtracted data–re-weighted MC comparisons using $B^\pm \rightarrow J/\psi K^\pm$ decays for two of the most powerful separation variables: (a) L_{xy} and (b) $I_{0.7}$. Uncertainties are statistical only. The lower graph in each case shows the data/MC ratio.

Table 3

Optimal selection variable cuts for the four-variables scan, and resulting analysis performance in terms of signal acceptance times efficiency (ϵ_{sig}), background yield in the signal region (N_{bkg}) and the estimator \mathcal{P} .

$ \alpha_{2D} $	ct	$I_{0.7}$	Δm	ϵ_{sig}	N_{bkg}	\mathcal{P}
< 0.03	> 0.3 mm	> 0.83	± 105 MeV	0.040	9 ± 2	0.010

ples in Section 3.3 (corresponding to the signal efficiency defined for $|\eta^B| < 2.5$ and $p_T^B > 8.0$ GeV) and the background yield for a given set of cuts. The extraction of N_{bkg} is performed by sideband interpolation as described in Section 5. The coefficient a was determined by the confidence level (CL) sought in the analysis, with $a = 2$ for a 95% CL limit. This quantity is specifically designed to optimize the performance of a frequentist limit determination in a counting analysis [30].

First, a simplified optimization procedure was performed on a small set of variables that includes: $|\alpha_{2D}|$, $I_{0.7}$, ct , and width $\pm \Delta m$ of the search window centred around the B_s^0 mass (rounded to 5366 MeV). A four-dimensional scan was performed on the four variables, using odd-numbered events in the sidebands. The optimal selection cuts are shown in Table 3, where the signal efficiency $\mathcal{A}_{\mu^+\mu^-} - \epsilon_{\mu^+\mu^-}$, the background estimated from sidebands interpolation and the value of \mathcal{P} are also given. This selection serves as a benchmark for the optimization of the multivariate analysis described in Section 3.4.2.

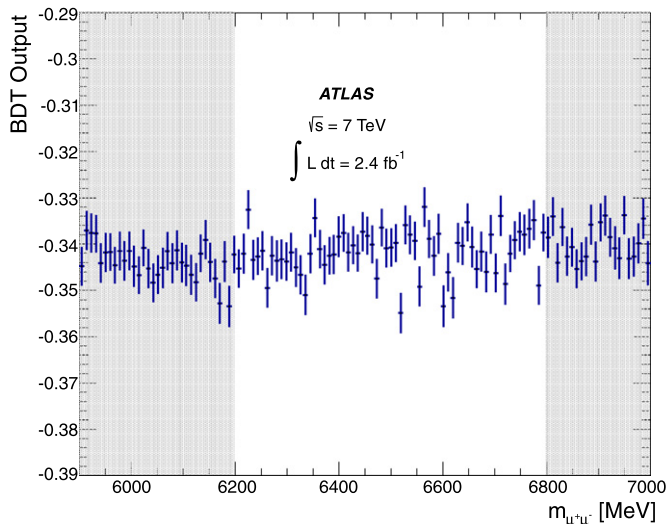


Fig. 4. Mean and RMS (error bars) of the BDT output in bins of di-muon invariant mass, for background events in the region 5900 to 7000 MeV, with the 6200 to 6800 MeV region not used in the training of the classifier. The BDT used is the one trained for the search of the fictitious 6500 MeV signal.

3.4.1. Categories of invariant-mass resolution

The ability to resolve a small $B_s^0 \rightarrow \mu^+ \mu^-$ signal from the continuum background depends on the width Δm of the search region and is therefore affected by the resolution. The latter varies considerably over different sub-samples of muon pairs measured by ATLAS, due to the increase in multiple scattering and the decrease of the magnetic field integral at large values of $|\eta|$. The non-resonant background invariant-mass distribution was observed to be relatively independent of η . As a consequence, different mass-resolution categories correspond to different signal-to-background conditions.

In the statistical analysis, regions of different mass resolution and hence signal-to-background ratio were separated in order to optimize them independently. The sample was separated into three categories, defined by the larger pseudorapidity value $|\eta|_{\max}$ of the two muons in each event. The three categories were defined by the intervals $|\eta|_{\max} = 0-1$, $1-1.5$ and $1.5-2.5$. The corresponding average values of the mass resolution are approximately 60, 80 and 110 MeV, respectively. The relative population of each interval, in $B_s^0 \rightarrow \mu^+ \mu^-$ signal MC, amounts to 51%, 24% and 25%.

The same classification, based on $|\eta|_{\max}$, was used for the reference channel $B^\pm \rightarrow J/\psi K^\pm$, and separate values of the acceptance-times-efficiency ratio were obtained for each category, as discussed in Section 4.1.

3.4.2. Multivariate selection

The selection with optimal cuts was used to validate the multivariate analysis tool used for the final results. The TMVA package [31] implementation of Boosted Decision Trees (BDT) was found to have the best performance and was selected for this analysis. As a first step, it was verified that for fixed values of Δm , the optimal BDT corresponds to selections in the variables α_{2D} , ct and $I_{0.7}$ directly comparable to those obtained with the cuts shown in Table 3. Next, the discriminating variables of Table 2 were introduced one-by-one into the BDT, verifying that the multivariate optimization increased the signal efficiency and the value of \mathcal{P} . With the BDT approach the \mathcal{P} estimator improved from $\mathcal{P} = 0.010$ found in the simplified optimization to $\mathcal{P} = 0.016$.

In order to avoid biases in the background interpolation, the BDT selection should be insensitive to the mass of the muon pair. The BDT inputs have no correlation with the invariant mass.

Table 4

BDT output and Δm cuts for each mass-resolution category, optimized according to the method described in the text.

$ \eta _{\max}$ range	0–1.0	1.0–1.5	1.5–2.5
Invariant-mass window [MeV]	± 116	± 133	± 171
BDT output threshold	0.234	0.245	0.270

Residual correlations in the BDT output were studied through the search for a fictitious decay $X \rightarrow \mu^+ \mu^-$ with $m_X = 6500$ MeV. A Monte Carlo sample was used to provide reference signal events, while data in the mass intervals 5900 to 6200 MeV and 6800 to 7000 MeV were used as background. The BDT training and selection optimization were consistently performed on odd-numbered events. Fig. 4 shows the BDT output as a function of the di-muon mass, over the sideband regions and the fictitious signal region (6200 to 6800 MeV), which was not used in the optimization. No significant mass dependence was observed.

The optimization of the multivariate analysis was performed in the six-dimensional space of Δm and the BDT output cuts for each of the mass-resolution categories. The independence of the BDT output on $m_{\mu^+ \mu^-}$ and the complementarity of the samples allow the factorization of the individual cut efficiencies. Each efficiency curve was interpolated with analytical models, allowing the numerical maximization of \mathcal{P} and yielding the optimal cuts reported in Table 4.

4. Single event sensitivity ingredients

4.1. Relative acceptance and efficiency

The ratio of the acceptance times efficiency products for the charged and neutral decays

$$R_{A\epsilon} = (A_{J/\psi K} \epsilon_{J/\psi K}) / (A_{\mu^+ \mu^-} \epsilon_{\mu^+ \mu^-})$$

is required for the determination of the SES (Eq. (1)). The same BDT, trained on the B_s^0 signal MC sample and di-muon data sidebands, was used to select both decay modes.

The uncertainty on $R_{A\epsilon}$ is affected by differences between data and MC in the distributions of the discriminating variables. Such differences are reduced by the data-driven corrections applied to the MC B -meson kinematics. Furthermore, only deviations that act incoherently between the signal and the reference channel contribute to the uncertainty on $R_{A\epsilon}$. These effects were studied by observing the change in the relative efficiency of the BDT selection when the simulated events were re-weighted by the data-to-MC ratio of the distributions of the most sensitive variables in $B^\pm \rightarrow J/\psi K^\pm$ events. The procedure was performed with the cut on the BDT output fixed at the optimal value for each of the three event categories. Conservatively, the corresponding variations in $R_{A\epsilon}$ were combined linearly and taken as systematic uncertainties.

Due to large correlations between L_{xy} , χ_{xy}^2 and ct -significance, correcting for the differences in L_{xy} between data and simulation was found to also effectively remove differences in the other two variables. Therefore only L_{xy} was considered, since it induced the largest deviation in $R_{A\epsilon}$. Differences in the η and p_T distributions of the final state particles, the hit multiplicity in the Pixel detector, and the multiplicity of reconstructed primary vertices were included in the systematic uncertainty evaluation.

Fig. 5 shows the distribution of the BDT output for MC samples of $B_s^0 \rightarrow \mu^+ \mu^-$ and $B^\pm \rightarrow J/\psi K^\pm$ decays, with a signal-background comparison for $B_s^0 \rightarrow \mu^+ \mu^-$ and a sideband-subtracted data-MC comparison for $B^\pm \rightarrow J/\psi K^\pm$. As shown in

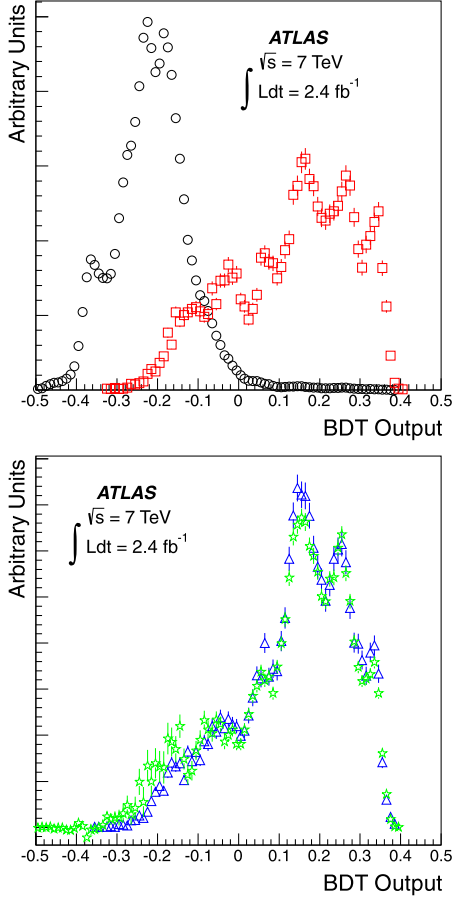


Fig. 5. Distributions of the response of the BDT classifier. Top: $B_s^0 \rightarrow \mu^+ \mu^-$ MC sample (squares) and data sidebands (circles); bottom: $B^\pm \rightarrow J/\psi K^\pm$ events from tuned MC samples (triangles) and sideband-subtracted data (stars).

Table 5

Values of the acceptance-times-efficiency ratio $R_{A\epsilon}$ between reference and search channel, shown separately for the different categories in mass resolution.

$ \eta _{\max}$ range	$R_{A\epsilon}^i$	Δ % stat.	Δ % syst.
0–1.0	0.274	3.1	3.1
1.0–1.5	0.202	4.8	5.5
1.5–2.5	0.143	5.3	5.9

Table 4, the selection required the BDT output to exceed 0.23–0.27, depending on the mass-resolution category. The systematic uncertainties induce a fractional change in the number of events passing the BDT cut varying between 10% and 20% depending on the category. This change is highly correlated between the two channels: the corresponding variation on the efficiency ratio is 0.6%, which was taken as a systematic uncertainty and is smaller than the $\pm 2.3\%$ error due to the finite MC statistics.

The value of $R_{A\epsilon}$ and its systematic uncertainties (shown in Table 5) were derived separately in the three mass-resolution categories. The MC-based efficiency was compared with that from $B^\pm \rightarrow J/\psi K^\pm$ data, computing the efficiency of the BDT cut relative to the preselection. The results are of similar precision and fully consistent: $0.258 \pm 0.013(\text{stat})$ for the data and $0.234 \pm 0.014(\text{stat}) \pm 0.011(\text{syst})$ for MC.

Additional smaller contributions to the uncertainty on $R_{A\epsilon}$ are due to the data–MC discrepancy in vertex reconstruction efficiency ($\pm 2\%$) [24], the uncertainty on the absolute K^\pm reconstruction efficiency as derived from simulation of the $B^\pm \rightarrow J/\psi K^\pm$ reference

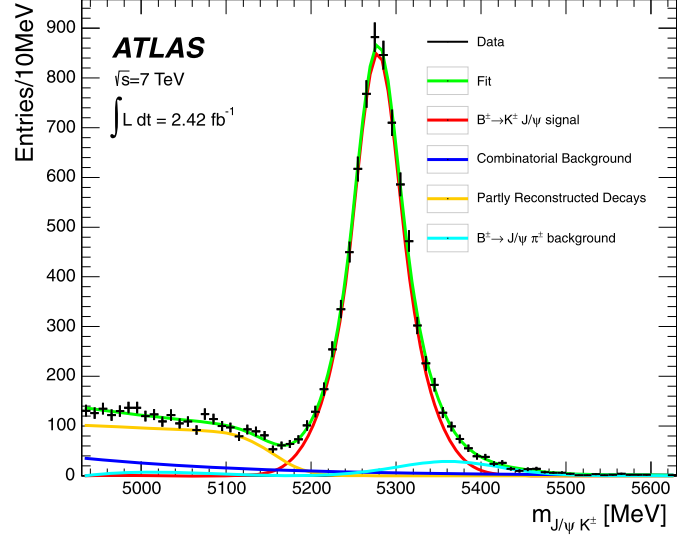


Fig. 6. $J/\psi K^\pm$ mass distribution for all the B^\pm candidates from even-numbered events passing all the selection cuts, merged for illustration purposes. Curves in the plot correspond to the various fit components: two Gaussians with a common mean for the main peak, a single Gaussian with higher mean for the $B^\pm \rightarrow J/\psi \pi^\pm$ decay, a falling exponential for the continuum background and an exponential function multiplying a complementary error function for the partially reconstructed decays.

Table 6

Event yield for even-numbered candidates in the reference channel.

$ \eta _{\max}$ range	0–1.0	1.0–1.5	1.5–2.5
$B^\pm \rightarrow J/\psi K^\pm \rightarrow \mu^+ \mu^- K^\pm$	4300	1410	1130
statistical uncertainty	$\pm 1.6\%$	$\pm 2.8\%$	$\pm 3.0\%$
systematic uncertainty	$\pm 2.9\%$	$\pm 7.4\%$	$\pm 14.1\%$

channel ($\pm 5\%$) and asymmetry differences in detector response to K^+ and K^- mesons ($\pm 1\%$).

4.2. $B^\pm \rightarrow J/\psi K^\pm$ event yield

The reference channel yield $N_{J/\psi K^\pm}$ was determined from a binned likelihood fit to the invariant-mass distribution of the $\mu^+ \mu^- K^\pm$ system, performed in the mass range 4930–5630 MeV. To avoid any bias induced by the DD re-weighting of the MC samples discussed in Section 3.3, only even-numbered events were used in the extraction of the $B^\pm \rightarrow J/\psi K^\pm$ event yield. The B^\pm signal was modelled with two Gaussian distributions of equal mean value. The background was modelled with the sum of: (a) an exponential function for the continuum combinatorial background; (b) an exponential function multiplied by a complementary error function describing the low-mass ($m < 5200$ MeV) contribution for partially reconstructed decays (such as $B \rightarrow J/\psi K^*$, $B \rightarrow J/\psi K(1270)$ and $B \rightarrow \chi_c K$); and (c) a Gaussian function for the background from $B^\pm \rightarrow J/\psi \pi^\pm$. Fig. 6 shows the invariant-mass distribution and the result of the fit for the selected data sample.

All parameters describing the signal and background were determined from the fit, with the exception of the mass and the width of the last component (c), which were obtained from simulation. The fit was performed for each of the three categories of mass resolution.

Systematic uncertainties affecting the extracted reference yield were estimated by varying the fit model: use of different bin sizes (10 or 25 MeV and unbinned), different models for signal and continuum background, inclusion of event-wise di-muon mass resolution. The resulting B^\pm yields are given with their statistical and systematic uncertainties in Table 6.

5. Inputs to the limit extraction

The evaluation of the SES requires as input the combined branching fraction for the reference channel $B^\pm \rightarrow J/\psi K^\pm \rightarrow \mu^+ \mu^- K^\pm$, which is $(6.01 \pm 0.21) \times 10^{-5}$ [20]. The relative production rate of B_s^0 relative to B^\pm f_s/f_u is 0.267 ± 0.021 [22], assuming $f_u = f_d$ (following Ref. [21]) and no kinematic dependence of f_s/f_u . The ratio of acceptance-times-efficiency is discussed in Section 4 and presented in Table 5. The branching fractions uncertainties, those on f_u/f_s , together with those mentioned in the last paragraph of Section 4.1, were treated coherently in the three categories of mass resolution.

In each mass-resolution category the $B_s^0 \rightarrow \mu^+ \mu^-$ signal yield $N_{\mu^+ \mu^-}$ was obtained from the number of events observed in the search window, the number of background events in the sidebands, and the small amount of resonant background discussed in Section 3.1. The expected ratio of the background events in the sidebands to those in the search window is described by the parameter R_i^{bkg} , which depends on the width of the invariant-mass interval and on the fraction of events from the sidebands used for the interpolation. The former varies according to the mass-resolution category, and the latter is equal to 50%, corresponding to the even-numbered events in the data collection. Uncertainties in the mass dependence of the continuum background produced a $\pm 4\%$ systematic error in the value of R_i^{bkg} , evaluated by studying the variation of R_i^{bkg} for different BDT output cuts and background interpolation models. The systematic variation accounts also for additional background components in the low mass sidebands (e.g. partially reconstructed B decays). This uncertainty was treated coherently in the three mass-resolution categories.

The values of the SES are given in Table 7 which also shows the values of the parameters R_i^{bkg} , the background counts in the sidebands,² the resonant background, and finally the observed number of events in the search region, as found after unblinding. Fig. 7 shows the invariant-mass distribution of the selected candidates in data, for the three mass categories, together with the signal projections as obtained from MC assuming $\text{BR}(B_s^0 \rightarrow \mu^+ \mu^-) = 3.5 \times 10^{-8}$ (i.e. approximately 10 times the SM expectation).

6. Branching fraction limits

The upper limit on the $B_s^0 \rightarrow \mu^+ \mu^-$ branching fraction was obtained by means of an implementation [32] of the CL_s method [33]. The extraction was based on the likelihood:

$$\begin{aligned} \mathcal{L} = & \text{Gauss}(\epsilon_{\text{obs}} | \epsilon, \sigma_\epsilon) \times \text{Gauss}(R_{\text{obs}}^{\text{bkg}} | R^{\text{bkg}}, \sigma_{R^{\text{bkg}}}) \\ & \times \prod_{i=1}^{N_{\text{bin}}} \text{Poisson}(N_i^{\text{obs}} | \epsilon \epsilon_i \text{BR} + N_i^{\text{bkg}} + N_i^{B \rightarrow hh}) \\ & \times \text{Poisson}(N_{\text{obs},i}^{\text{bkg}} | R^{\text{bkg}} R_i^{\text{bkg}} N_i^{\text{bkg}}) \\ & \times \text{Gauss}(\epsilon_{\text{obs},i} | \epsilon_i, \sigma_{\epsilon_i}). \end{aligned}$$

For each mass-resolution category, the likelihood contains Poisson distributions for the event counts in the search and sideband regions and a Gaussian distribution for the relative efficiency ϵ_i . Two additional Gaussians describe the coherent systematic uncertainties in R^{bkg} and in the SES. The mean of the Poisson distribution in the search region is equal to the sum of the B_s^0 branching frac-

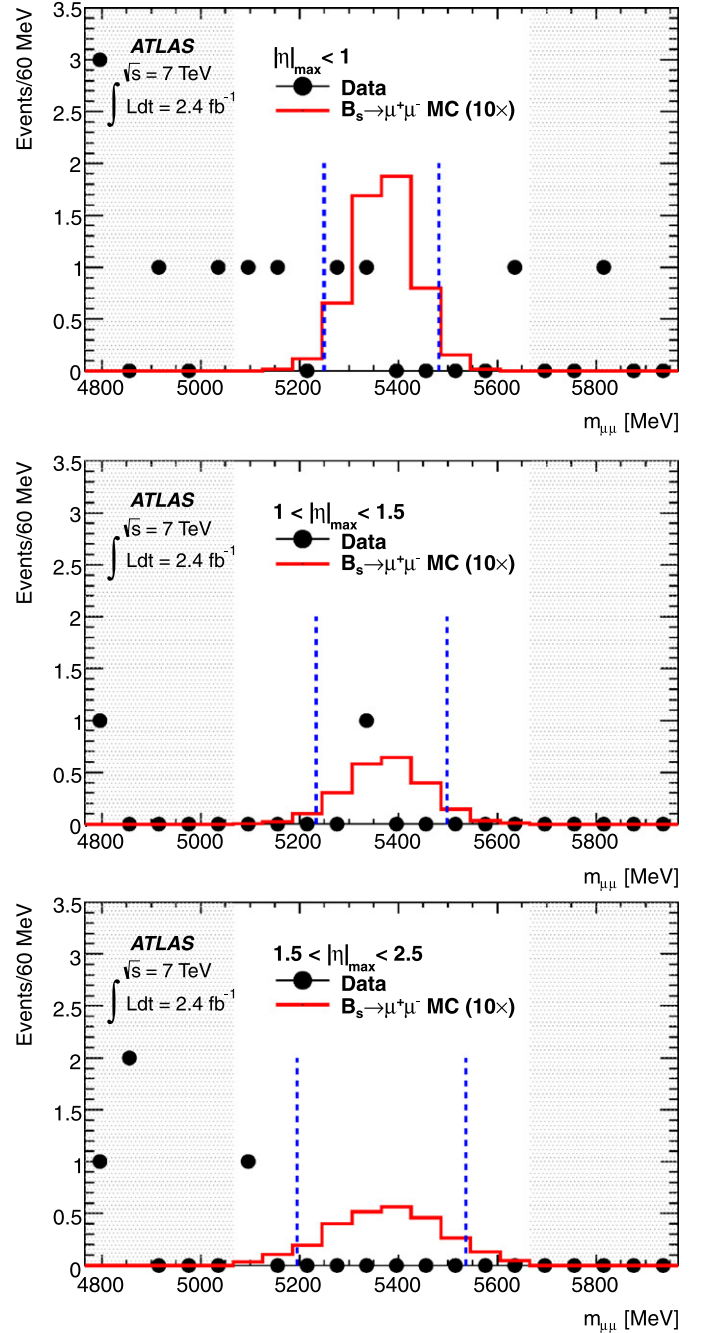


Fig. 7. Invariant-mass distribution of candidates in data. For each mass-resolution category (top to bottom) each plot shows the invariant-mass distribution for the selected candidates in data (dots), the signal (continuous line) as predicted by MC assuming $\text{BR}(B_s^0 \rightarrow \mu^+ \mu^-) = 3.5 \times 10^{-8}$, and two dashed vertical lines corresponding to the optimized Δm cut. The grey areas correspond to the sidebands used in the analysis.

tion (scaled by the normalization and relative efficiency parameters), the continuum background and the resonant background. The mean of the Poisson distribution in the sidebands is equal to the background scaled by R^{bkg} . The parameters σ_ϵ (σ_{ϵ_i}), $\sigma_{R^{\text{bkg}}}$ ($\sigma_{R_i^{\text{bkg}}}$) account for the correlated (uncorrelated) uncertainties in the SES and the background scaling factor. In this analysis the uncertainties on R_i^{bkg} are negligible, with $R^{\text{bkg}} = 1.00 \pm 0.04$. All input parameters are summarized in Table 7.

The expected limits were obtained by setting the counts in the search region equal to the interpolated background plus the

² For comparison, the number of odd-numbered events observed in the sidebands, which is expected to be biased due to the use of the same sample in selection optimization and BDT training, was found to be equal to one event in each of the three mass-resolution categories.

Table 7

Single event sensitivity and event counts in the three mass-resolution categories. The second and third lines report how the $SES = (\epsilon\epsilon_i)^{-1}$ was split between a coefficient common to all bins, and the per-bin component. The table does not include the additional common uncertainties corresponding the sources mentioned in the last paragraph of Section 4.1 ($\pm 5.5\%$ in R_{Ae}^i) and to the parameterization of the mass dependence of the continuum background ($\pm 4\%$ in R_i^{bkg}).

$ \eta _{\max}$ range	0–1.0	1.0–1.5	1.5–2.5
$SES = (\epsilon\epsilon_i)^{-1} [10^{-8}]$	0.71	1.6	1.4
$\epsilon = (f_s/f_u)/BR(B^\pm \rightarrow J/\psi K^\pm \rightarrow \mu^+\mu^-K^\pm) [10^3]$		4.45 ± 0.38	
$\epsilon_i = N_i^{B^\pm \rightarrow J/\psi K^\pm}/R_{Ae}^i [10^4]$	3.14 ± 0.17	1.40 ± 0.15	1.58 ± 0.26
bkg. scaling factor R_i^{bkg}	1.29	1.14	0.88
sideband count $N_{obs,i}^{bkg}$ (even numbered events)	5	0	2
expected resonant bkg. $N_i^{B \rightarrow hh}$	0.10	0.06	0.08
search region count N_i^{obs}	2	1	0

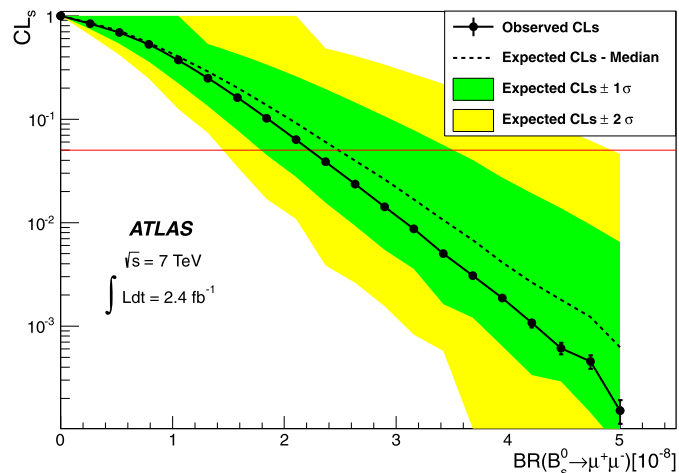


Fig. 8. Observed CL_s (circles) as a function of $BR(B_s^0 \rightarrow \mu^+\mu^-)$. The 95% CL limit is indicated by the horizontal (red) line. The dark (green) and light (yellow) bands correspond to $\pm 1\sigma$ and $\pm 2\sigma$ fluctuations on the expectation (dashed line), based on the number of observed events in the signal and sideband regions.

small resonant background, before the unblinding of the signal region. A median expected limit of $2.3_{-0.5}^{+1.0} \times 10^{-8}$ at 95% CL was obtained, where the range encloses 68% of the background-only pseudo-experiments.

For comparison the mass-resolution categories were merged and the selection optimization was performed on the merged sample. In this case eight events were found in the sidebands, resulting in a branching fraction limit of $2.9_{-0.8}^{+1.3} \times 10^{-8}$ at 95% CL. This test confirms the expectation of a more sensitive analysis when separate mass-resolution categories are used.

The background counts found in odd-numbered events were used to assess the magnitude of the bias that would be caused by using the same sample for selection optimization and the estimation of N^{bkg} . The expected limit obtained using the same sample for optimization and signal extraction is 1.7×10^{-8} , about 30% smaller than the limit presented in this Letter, for which independent samples were used for optimization and for signal extraction. The observed bias is consistent with simulation-based assessments of this effect.

Fig. 8 shows the behaviour of the observed CL_s for different tested values of the $B_s^0 \rightarrow \mu^+\mu^-$ branching fraction, computed with 300 000 toy MC simulations per point. The observed limit is $< 2.2(1.9) \times 10^{-8}$ at 95% (90%) CL. The p -values for the background-only hypothesis and for background plus SM prediction [1,2] are 44% and 35%, respectively.

Despite the difference between the total numbers of observed and interpolated background events (equal to 3 and 6.5, respectively), the interplay of the event counts observed in the three

mass-resolution categories produced an observed CL_s limit close to the expected value.

7. Conclusions

A limit on the branching fraction $BR(B_s^0 \rightarrow \mu^+\mu^-)$ is set using 2.4 fb^{-1} of integrated luminosity collected in 2011 by the ATLAS detector. The process $B^\pm \rightarrow J/\psi K^\pm$, with $J/\psi \rightarrow \mu^+\mu^-$, is used as a reference channel for the normalization of integrated luminosity, acceptance and efficiency. The final selection is based on a multivariate analysis performed on three categories of events determined according to their mass resolution, yielding a limit of $BR(B_s^0 \rightarrow \mu^+\mu^-) < 2.2(1.9) \times 10^{-8}$ at 95% (90%) CL.

Acknowledgements

We thank CERN for the very successful operation of the LHC, as well as the support staff from our institutions without whom ATLAS could not be operated efficiently.

We acknowledge the support of ANPCyT, Argentina; YerPhI, Armenia; ARC, Australia; BMWF, Austria; ANAS, Azerbaijan; SSTC, Belarus; CNPq and FAPESP, Brazil; NSERC, NRC and CFI, Canada; CERN; CONICYT, Chile; CAS, MOST and NSFC, China; COLCIENCIAS, Colombia; MSMT CR, MPO CR and VSC CR, Czech Republic; DNRF, DNSRC and Lundbeck Foundation, Denmark; EPLANET and ERC, European Union; IN2P3–CNRS, CEA–DSM/IRFU, France; GNAS, Georgia; BMBF, DFG, HGF, MPG and AvH Foundation, Germany; GSRT, Greece; ISF, MINERVA, GIF, DIP and Benoziyo Center, Israel; INFN, Italy; MEXT and JSPS, Japan; CNRST, Morocco; FOM and NWO, Netherlands; RCN, Norway; MNiSW, Poland; GRICES and FCT, Portugal; MERYS (MECTS), Romania; MES of Russia and ROSATOM, Russian Federation; JINR; MSTB, Serbia; MSSR, Slovakia; ARRS and MVZT, Slovenia; DST/NRF, South Africa; MICINN, Spain; SRC and Wallenberg Foundation, Sweden; SER, SNSF and Cantons of Bern and Geneva, Switzerland; NSC, Taiwan; TAEK, Turkey; STFC, the Royal Society and Leverhulme Trust, United Kingdom; DOE and NSF, United States of America.

The crucial computing support from all WLCG partners is acknowledged gratefully, in particular from CERN and the ATLAS Tier-1 facilities at TRIUMF (Canada), NDGF (Denmark, Norway, Sweden), CC-IN2P3 (France), KIT/GridKA (Germany), INFN-CNAF (Italy), NL-T1 (Netherlands), PIC (Spain), ASGC (Taiwan), RAL (UK) and BNL (USA) and in the Tier-2 facilities worldwide.

Open access

This article is published Open Access at sciencedirect.com. It is distributed under the terms of the Creative Commons Attribution License 3.0, which permits unrestricted use, distribution, and reproduction in any medium, provided the original authors and source are credited.

References

- [1] A.J. Buras, G. Isidori, P. Paradisi, Phys. Lett. B 694 (2011) 402.
 [2] A.J. Buras, Acta Phys. Polon. B 41 (2010) 2487.
 [3] UTfit Collaboration, M. Bona, et al., PoS (EPS-HEP2011) (2011) 185.
 [4] CKMfitter Collaboration, J. Charles, et al., Eur. Phys. J. C 41 (2005) 1.
 [5] L.J. Hall, R. Rattazzi, U. Sarid, Phys. Rev. D 50 (1994) 7048.
 [6] C. Hamzaoui, M. Pospelov, M. Toharia, Phys. Rev. D 59 (1999) 095005.
 [7] K.S. Babu, C.F. Kolda, Phys. Rev. Lett. 84 (2000) 228.
 [8] S. Choudhury, A.S. Cornell, N. Gaur, G.C. Joshi, Int. J. Mod. Phys. A 21 (2006) 2617.
 [9] J. Parry, Nucl. Phys. B 760 (2007) 38.
 [10] J.R. Ellis, K.A. Olive, Y. Santoso, V.C. Spanos, JHEP 0605 (2006) 063.
 [11] J.R. Ellis, J.S. Lee, A. Pilaftsis, Phys. Rev. D 76 (2007) 115011.
 [12] S. Davidson, S. Descotes-Genon, JHEP 1011 (2010) 073.
 [13] D0 Collaboration, V. Abazov, et al., Phys. Lett. B 693 (2010) 539.
 [14] CDF Collaboration, T. Aaltonen, et al., Phys. Rev. Lett. 107 (2011) 239903.
 [15] CMS Collaboration, Phys. Rev. Lett. 107 (2011) 191802.
 [16] CMS Collaboration, Search for $B_s^0 \rightarrow \mu\mu$ and $B^0 \rightarrow \mu\mu$ decays, arXiv:1203.3976.
 [17] LHCb Collaboration, R. Aaij, et al., Phys. Lett. B 708 (2012) 55.
 [18] LHCb Collaboration, R. Aaij, et al., Strong constraints on the rare decays $B_s^0 \rightarrow \mu^+\mu^-$ and $B^0 \rightarrow \mu^+\mu^-$, arXiv:1203.4493.
 [19] ATLAS Collaboration, JINST 3 (2008) S08003.
 [20] Particle Data Group, K. Nakamura, et al., J. Phys. G 37 (7A) (2010) 075021.
 [21] Heavy Flavor Averaging Group, D. Asner, et al., Averages of b -hadron, c -hadron, and τ -lepton properties, arXiv:1010.1589.
 [22] LHCb Collaboration, R. Aaij, et al., Phys. Rev. D 85 (2012) 032008.
 [23] ATLAS Collaboration, Eur. Phys. J. C 72 (2012) 1849.
 [24] ATLAS Collaboration, New J. Phys. 13 (2011) 053033.
 [25] T. Sjostrand, S. Mrenna, P.Z. Skands, JHEP 0605 (2006) 026.
 [26] A. Buckley, ATLAS Monte Carlo generator tunes to LHC data, in: Nuclear Science Symposium Conference Record (NSS/MIC), 2010 IEEE, 2010, pp. 167–173.
 [27] GEANT4 Collaboration, S. Agostinelli, et al., Nucl. Instrum. Meth. A 506 (2003) 250303.
 [28] CDF Collaboration, T. Aaltonen, et al., Evidence for the charmless annihilation decay mode $B_s^0 \rightarrow \pi^+\pi^-$, arXiv:1111.0485.
 [29] ATLAS Collaboration, Muon reconstruction performance, ATLAS-CONF-2010-064.
 [30] G. Punzi, Sensitivity of searches for new signals and its optimization, arXiv:physics/0308063.
 [31] A. Hoecker, P. Speckmayer, J. Stelzer, J. Therhaag, E. von Toerne, H. Voss, PoS ACAT (2007) 040.
 [32] T. Junk, Nucl. Instrum. Meth. A 434 (1999) 435.
 [33] A.L. Read, J. Phys. G 28 (2002) 2693.

ATLAS Collaboration

G. Aad⁴⁸, B. Abbott¹¹¹, J. Abdallah¹¹, S. Abdel Khalek¹¹⁵, A.A. Abdelalim⁴⁹, O. Abdinov¹⁰, B. Abi¹¹², M. Abolins⁸⁸, O.S. AbouZeid¹⁵⁸, H. Abramowicz¹⁵³, H. Abreu¹³⁶, E. Acerbi^{89a,89b}, B.S. Acharya^{164a,164b}, L. Adamczyk³⁷, D.L. Adams²⁴, T.N. Addy⁵⁶, J. Adelman¹⁷⁶, S. Adomeit⁹⁸, P. Adragna⁷⁵, T. Adye¹²⁹, S. Aefsky²², J.A. Aguilar-Saavedra^{124b,a}, M. Aharrouche⁸¹, S.P. Ahlen²¹, F. Ahles⁴⁸, A. Ahmad¹⁴⁸, M. Ahsan⁴⁰, G. Aielli^{133a,133b}, T. Akdogan^{18a}, T.P.A. Åkesson⁷⁹, G. Akimoto¹⁵⁵, A.V. Akimov⁹⁴, A. Akiyama⁶⁶, M.S. Alam¹, M.A. Alam⁷⁶, J. Albert¹⁶⁹, S. Albrand⁵⁵, M. Aleksa²⁹, I.N. Aleksandrov⁶⁴, F. Alessandria^{89a}, C. Alexa^{25a}, G. Alexander¹⁵³, G. Alexandre⁴⁹, T. Alexopoulos⁹, M. Alhroob^{164a,164c}, M. Aliev¹⁵, G. Alimonti^{89a}, J. Alison¹²⁰, B.M.M. Allbrooke¹⁷, P.P. Allport⁷³, S.E. Allwood-Spiers⁵³, J. Almond⁸², A. Aloisio^{102a,102b}, R. Alon¹⁷², A. Alonso⁷⁹, B. Alvarez Gonzalez⁸⁸, M.G. Alviggi^{102a,102b}, K. Amako⁶⁵, C. Amelung²², V.V. Ammosov¹²⁸, A. Amorim^{124a,b}, N. Amram¹⁵³, C. Anastopoulos²⁹, L.S. Ancu¹⁶, N. Andari¹¹⁵, T. Andeen³⁴, C.F. Anders²⁰, G. Anders^{58a}, K.J. Anderson³⁰, A. Andreazza^{89a,89b}, V. Andrei^{58a}, X.S. Anduaga⁷⁰, A. Angerami³⁴, F. Anghinolfi²⁹, A. Anisenkov¹⁰⁷, N. Anjos^{124a}, A. Annovi⁴⁷, A. Antonaki⁸, M. Antonelli⁴⁷, A. Antonov⁹⁶, J. Antos^{144b}, F. Anulli^{132a}, S. Aoun⁸³, L. Aperio Bella⁴, R. Apolle^{118,c}, G. Arabidze⁸⁸, I. Aracena¹⁴³, Y. Arai⁶⁵, A.T.H. Arce⁴⁴, S. Arfaoui¹⁴⁸, J.-F. Arguin¹⁴, E. Arik^{18a,*}, M. Arik^{18a}, A.J. Armbruster⁸⁷, O. Arnaez⁸¹, V. Arnal⁸⁰, C. Arnault¹¹⁵, A. Artamonov⁹⁵, G. Artoni^{132a,132b}, D. Arutinov²⁰, S. Asai¹⁵⁵, R. Asfandiyarov¹⁷³, S. Ask²⁷, B. Åsman^{146a,146b}, L. Asquith⁵, K. Assamagan²⁴, A. Astbury¹⁶⁹, B. Aubert⁴, E. Auge¹¹⁵, K. Augsten¹²⁷, M. Auresseau^{145a}, G. Avolio¹⁶³, R. Avramidou⁹, D. Axen¹⁶⁸, G. Azuelos^{93,d}, Y. Azuma¹⁵⁵, M.A. Baak²⁹, G. Baccaglioni^{89a}, C. Bacci^{134a,134b}, A.M. Bach¹⁴, H. Bachacou¹³⁶, K. Bachas²⁹, M. Backes⁴⁹, M. Backhaus²⁰, E. Badescu^{25a}, P. Bagnaia^{132a,132b}, S. Bahinipati², Y. Bai^{32a}, D.C. Bailey¹⁵⁸, T. Bain¹⁵⁸, J.T. Baines¹²⁹, O.K. Baker¹⁷⁶, M.D. Baker²⁴, S. Baker⁷⁷, E. Banas³⁸, P. Banerjee⁹³, Sw. Banerjee¹⁷³, D. Banfi²⁹, A. Bangert¹⁵⁰, V. Bansal¹⁶⁹, H.S. Bansil¹⁷, L. Barak¹⁷², S.P. Baranov⁹⁴, A. Barbaro Galtieri¹⁴, T. Barber⁴⁸, E.L. Barberio⁸⁶, D. Barberis^{50a,50b}, M. Barbero²⁰, D.Y. Bardin⁶⁴, T. Barillari⁹⁹, M. Barisonzi¹⁷⁵, T. Barklow¹⁴³, N. Barlow²⁷, B.M. Barnett¹²⁹, R.M. Barnett¹⁴, A. Baroncelli^{134a}, G. Barone⁴⁹, A.J. Barr¹¹⁸, F. Barreiro⁸⁰, J. Barreiro Guimarães da Costa⁵⁷, P. Barrillon¹¹⁵, R. Bartoldus¹⁴³, A.E. Barton⁷¹, V. Bartsch¹⁴⁹, R.L. Bates⁵³, L. Batkova^{144a}, J.R. Batley²⁷, A. Battaglia¹⁶, M. Battistin²⁹, F. Bauer¹³⁶, H.S. Bawa^{143,e}, S. Beale⁹⁸, T. Beau⁷⁸, P.H. Beauchemin¹⁶¹, R. Beccherle^{50a}, P. Bechtel²⁰, H.P. Beck¹⁶, S. Becker⁹⁸, M. Beckingham¹³⁸, K.H. Becks¹⁷⁵, A.J. Beddall^{18c}, A. Beddall^{18c}, S. Bedikian¹⁷⁶, V.A. Bednyakov⁶⁴, C.P. Bee⁸³, M. Beger²⁴, S. Behar Harpaz¹⁵², P.K. Behera⁶², M. Beimforde⁹⁹, C. Belanger-Champagne⁸⁵, P.J. Bell⁴⁹, W.H. Bell⁴⁹, G. Bella¹⁵³, L. Bellagamba^{19a}, F. Bellina²⁹, M. Bellomo²⁹, A. Belloni⁵⁷, O. Beloborodova^{107,f}, K. Belotskiy⁹⁶, O. Beltramello²⁹, O. Benary¹⁵³, D. Benchekroun^{135a}, K. Bendtz^{146a,146b}, N. Benekos¹⁶⁵, Y. Benhammou¹⁵³, E. Benhar Noccioli⁴⁹, J.A. Benitez Garcia^{159b}, D.P. Benjamin⁴⁴, M. Benoit¹¹⁵, J.R. Bensinger²², K. Benslama¹³⁰, S. Bentvelsen¹⁰⁵, D. Berge²⁹,

E. Bergeas Kuutmann⁴¹, N. Berger⁴, F. Berghaus¹⁶⁹, E. Berglund¹⁰⁵, J. Beringer¹⁴, P. Bernat⁷⁷,
 R. Bernhard⁴⁸, C. Bernius²⁴, T. Berry⁷⁶, C. Bertella⁸³, A. Bertin^{19a,19b}, F. Bertolucci^{122a,122b},
 M.I. Besana^{89a,89b}, N. Besson¹³⁶, S. Bethke⁹⁹, W. Bhimji⁴⁵, R.M. Bianchi²⁹, M. Bianco^{72a,72b}, O. Biebel⁹⁸,
 S.P. Bieniek⁷⁷, K. Bierwagen⁵⁴, J. Biesiada¹⁴, M. Biglietti^{134a}, H. Bilokon⁴⁷, M. Bindi^{19a,19b}, S. Binet¹¹⁵,
 A. Bingul^{18c}, C. Bini^{132a,132b}, C. Biscarat¹⁷⁸, U. Bitenc⁴⁸, K.M. Black²¹, R.E. Blair⁵, J.-B. Blanchard¹³⁶,
 G. Blanchot²⁹, T. Blazek^{144a}, C. Blocker²², J. Blocki³⁸, A. Blondel⁴⁹, W. Blum⁸¹, U. Blumenschein⁵⁴,
 G.J. Bobbink¹⁰⁵, V.B. Bobrovnikov¹⁰⁷, S.S. Bocchetta⁷⁹, A. Bocci⁴⁴, C.R. Boddy¹¹⁸, M. Boehler⁴¹,
 J. Boek¹⁷⁵, N. Boelaert³⁵, J.A. Bogaerts²⁹, A. Bogdanchikov¹⁰⁷, A. Bogouch^{90,*}, C. Boehm^{146a}, J. Boehm¹²⁵,
 V. Boisvert⁷⁶, T. Bold³⁷, V. Boldea^{25a}, N.M. Bolnet¹³⁶, M. Bomben⁷⁸, M. Bona⁷⁵, M. Bondioli¹⁶³,
 M. Boonekamp¹³⁶, C.N. Booth¹³⁹, S. Bordini⁷⁸, C. Borer¹⁶, A. Borisov¹²⁸, G. Borisov⁷¹, I. Borjanovic^{12a},
 M. Borri⁸², S. Borroni⁸⁷, V. Bortolotto^{134a,134b}, K. Bos¹⁰⁵, D. Boscherini^{19a}, M. Bosman¹¹,
 H. Boterenbrood¹⁰⁵, D. Botterill¹²⁹, J. Bouchami⁹³, J. Boudreau¹²³, E.V. Bouhova-Thacker⁷¹,
 D. Boumediene³³, C. Bourdarios¹¹⁵, N. Bousson⁸³, A. Boveia³⁰, J. Boyd²⁹, I.R. Boyko⁶⁴, N.I. Bozhko¹²⁸,
 I. Bozovic-Jelisavcic^{12b}, J. Bracinik¹⁷, P. Branchini^{134a}, A. Brandt⁷, G. Brandt¹¹⁸, O. Brandt⁵⁴,
 U. Bratzler¹⁵⁶, B. Brau⁸⁴, J.E. Brau¹¹⁴, H.M. Braun¹⁷⁵, B. Brelrier¹⁵⁸, J. Bremer²⁹, K. Brendlinger¹²⁰,
 R. Brenner¹⁶⁶, S. Bressler¹⁷², D. Britton⁵³, F.M. Brochu²⁷, I. Brock²⁰, R. Brock⁸⁸, E. Brodet¹⁵³,
 F. Broggi^{89a}, C. Bromberg⁸⁸, J. Bronner⁹⁹, G. Brooijmans³⁴, W.K. Brooks^{31b}, G. Brown⁸², H. Brown⁷,
 P.A. Bruckman de Renstrom³⁸, D. Bruncko^{144b}, R. Bruneliere⁴⁸, S. Brunet⁶⁰, A. Bruni^{19a}, G. Bruni^{19a},
 M. Bruschi^{19a}, T. Buanes¹³, Q. Buat⁵⁵, F. Bucci⁴⁹, J. Buchanan¹¹⁸, P. Buchholz¹⁴¹, R.M. Buckingham¹¹⁸,
 A.G. Buckley⁴⁵, S.I. Buda^{25a}, I.A. Budagov⁶⁴, B. Budick¹⁰⁸, V. Büscher⁸¹, L. Bugge¹¹⁷, O. Bulekov⁹⁶,
 A.C. Bundock⁷³, M. Bunse⁴², T. Buran¹¹⁷, H. Burckhart²⁹, S. Burdin⁷³, T. Burgess¹³, S. Burke¹²⁹,
 E. Busato³³, P. Bussey⁵³, C.P. Buszello¹⁶⁶, B. Butler¹⁴³, J.M. Butler²¹, C.M. Buttar⁵³, J.M. Butterworth⁷⁷,
 W. Buttinger²⁷, S. Cabrera Urbán¹⁶⁷, D. Caforio^{19a,19b}, O. Cakir^{3a}, P. Calafiura¹⁴, G. Calderini⁷⁸,
 P. Calfayan⁹⁸, R. Calkins¹⁰⁶, L.P. Caloba^{23a}, R. Caloi^{132a,132b}, D. Calvet³³, S. Calvet³³, R. Camacho Toro³³,
 P. Camarri^{133a,133b}, D. Cameron¹¹⁷, L.M. Caminada¹⁴, S. Campana²⁹, M. Campanelli⁷⁷,
 V. Canale^{102a,102b}, F. Canelli^{30,g}, A. Canepa^{159a}, J. Cantero⁸⁰, L. Capasso^{102a,102b},
 M.D.M. Capeans Garrido²⁹, I. Caprini^{25a}, M. Caprini^{25a}, D. Capriotti⁹⁹, M. Capua^{36a,36b}, R. Caputo⁸¹,
 R. Cardarelli^{133a}, T. Carli²⁹, G. Carlino^{102a}, L. Carminati^{89a,89b}, B. Caron⁸⁵, S. Caron¹⁰⁴, E. Carquin^{31b},
 G.D. Carrillo Montoya¹⁷³, A.A. Carter⁷⁵, J.R. Carter²⁷, J. Carvalho^{124a,h}, D. Casadei¹⁰⁸, M.P. Casado¹¹,
 M. Cascella^{122a,122b}, C. Caso^{50a,50b,*}, A.M. Castaneda Hernandez^{173,i}, E. Castaneda-Miranda¹⁷³,
 V. Castillo Gimenez¹⁶⁷, N.F. Castro^{124a}, G. Cataldi^{72a}, P. Catastini⁵⁷, A. Catinaccio²⁹, J.R. Catmore²⁹,
 A. Cattai²⁹, G. Cattani^{133a,133b}, S. Caughron⁸⁸, P. Cavalleri⁷⁸, D. Cavalli^{89a}, M. Cavalli-Sforza¹¹,
 V. Cavasinni^{122a,122b}, F. Ceradini^{134a,134b}, A.S. Cerqueira^{23b}, A. Cerri²⁹, L. Cerrito⁷⁵, F. Cerutti⁴⁷,
 S.A. Cetin^{18b}, A. Chafaq^{135a}, D. Chakraborty¹⁰⁶, I. Chalupkova¹²⁶, K. Chan², B. Chapleau⁸⁵,
 J.D. Chapman²⁷, J.W. Chapman⁸⁷, E. Chareyre⁷⁸, D.G. Charlton¹⁷, V. Chavda⁸², C.A. Chavez Barajas²⁹,
 S. Cheatham⁸⁵, S. Chekanov⁵, S.V. Chekulaev^{159a}, G.A. Chelkov⁶⁴, M.A. Chelstowska¹⁰⁴, C. Chen⁶³,
 H. Chen²⁴, S. Chen^{32c}, X. Chen¹⁷³, A. Cheplakov⁶⁴, R. Cherkaoui El Moursli^{135e}, V. Chernyatin²⁴,
 E. Cheu⁶, S.L. Cheung¹⁵⁸, L. Chevalier¹³⁶, G. Chiefari^{102a,102b}, L. Chikovani^{51a}, J.T. Childers²⁹,
 A. Chilingarov⁷¹, G. Chiodini^{72a}, A.S. Chisholm¹⁷, R.T. Chislett⁷⁷, M.V. Chizhov⁶⁴, G. Choudalakis³⁰,
 S. Chouridou¹³⁷, I.A. Christidi⁷⁷, A. Christov⁴⁸, D. Chromek-Burckhart²⁹, M.L. Chu¹⁵¹, J. Chudoba¹²⁵,
 G. Ciapetti^{132a,132b}, A.K. Ciftci^{3a}, R. Ciftci^{3a}, D. Cinca³³, V. Cindro⁷⁴, C. Ciocca^{19a}, A. Ciochio¹⁴,
 M. Cirilli⁸⁷, M. Citterio^{89a}, M. Ciubancan^{25a}, A. Clark⁴⁹, P.J. Clark⁴⁵, W. Cleland¹²³, J.C. Clemens⁸³,
 B. Clement⁵⁵, C. Clement^{146a,146b}, Y. Coadou⁸³, M. Cobal^{164a,164c}, A. Coccaro¹³⁸, J. Cochran⁶³, P. Coe¹¹⁸,
 J.G. Cogan¹⁴³, J. Coggeshall¹⁶⁵, E. Cogneras¹⁷⁸, J. Colas⁴, A.P. Colijn¹⁰⁵, N.J. Collins¹⁷, C. Collins-Tooth⁵³,
 J. Collot⁵⁵, G. Colon⁸⁴, P. Conde Muiño^{124a}, E. Coniavitis¹¹⁸, M.C. Conidi¹¹, S.M. Consonni^{89a,89b},
 V. Consorti⁴⁸, S. Constantinescu^{25a}, C. Conta^{119a,119b}, G. Conti⁵⁷, F. Conventi^{102a,j}, M. Cooke¹⁴,
 B.D. Cooper⁷⁷, A.M. Cooper-Sarkar¹¹⁸, K. Copic¹⁴, T. Cornelissen¹⁷⁵, M. Corradi^{19a}, F. Corriveau^{85,k},
 A. Cortes-Gonzalez¹⁶⁵, G. Cortiana⁹⁹, G. Costa^{89a}, M.J. Costa¹⁶⁷, D. Costanzo¹³⁹, T. Costin³⁰, D. Côté²⁹,
 L. Courneyea¹⁶⁹, G. Cowan⁷⁶, C. Cowden²⁷, B.E. Cox⁸², K. Cranmer¹⁰⁸, F. Crescioli^{122a,122b},
 M. Cristinziani²⁰, G. Crosetti^{36a,36b}, R. Crupi^{72a,72b}, S. Crépe-Renaudin⁵⁵, C.-M. Cuciuc^{25a},
 C. Cuenca Almenar¹⁷⁶, T. Cuhadar Donszelmann¹³⁹, M. Curatolo⁴⁷, C.J. Curtis¹⁷, C. Cuthbert¹⁵⁰,
 P. Cwetanski⁶⁰, H. Czirr¹⁴¹, P. Czodrowski⁴³, Z. Czynzula¹⁷⁶, S. D'Auria⁵³, M. D'Onofrio⁷³,

A. D’Orazio ^{132a,132b}, C. Da Via ⁸², W. Dabrowski ³⁷, A. Dafinca ¹¹⁸, T. Dai ⁸⁷, C. Dallapiccola ⁸⁴, M. Dam ³⁵,
 M. Dameri ^{50a,50b}, D.S. Damiani ¹³⁷, H.O. Danielsson ²⁹, V. Dao ⁴⁹, G. Darbo ^{50a}, G.L. Darlea ^{25b},
 W. Davey ²⁰, T. Davidek ¹²⁶, N. Davidson ⁸⁶, R. Davidson ⁷¹, E. Davies ^{118,c}, M. Davies ⁹³, A.R. Davison ⁷⁷,
 Y. Davygora ^{58a}, E. Dawe ¹⁴², I. Dawson ¹³⁹, R.K. Daya-Ishmukhametova ²², K. De ⁷, R. de Asmundis ^{102a},
 S. De Castro ^{19a,19b}, S. De Cecco ⁷⁸, J. de Graat ⁹⁸, N. De Groot ¹⁰⁴, P. de Jong ¹⁰⁵, C. De La Taille ¹¹⁵,
 H. De la Torre ⁸⁰, F. De Lorenzi ⁶³, L. de Mora ⁷¹, L. De Nooij ¹⁰⁵, D. De Pedis ^{132a}, A. De Salvo ^{132a},
 U. De Sanctis ^{164a,164c}, A. De Santo ¹⁴⁹, J.B. De Vivie De Regie ¹¹⁵, G. De Zorzi ^{132a,132b}, W.J. Dearnaley ⁷¹,
 R. Debbe ²⁴, C. Debenedetti ⁴⁵, B. Dechenaux ⁵⁵, D.V. Dedovich ⁶⁴, J. Degenhardt ¹²⁰, C. Del Papa ^{164a,164c},
 J. Del Peso ⁸⁰, T. Del Prete ^{122a,122b}, T. Delemontex ⁵⁵, M. Deliyergiyev ⁷⁴, A. Dell’Acqua ²⁹, L. Dell’Asta ²¹,
 M. Della Pietra ^{102a,j}, D. della Volpe ^{102a,102b}, M. Delmastro ⁴, P.A. Delsart ⁵⁵, C. Deluca ¹⁴⁸, S. Demers ¹⁷⁶,
 M. Demichev ⁶⁴, B. Demirköz ^{11,l}, J. Deng ¹⁶³, S.P. Denisov ¹²⁸, D. Derendarz ³⁸, J.E. Derkaoui ^{135d},
 F. Derue ⁷⁸, P. Dervan ⁷³, K. Desch ²⁰, E. Devetak ¹⁴⁸, P.O. Deviveiros ¹⁰⁵, A. Dewhurst ¹²⁹, B. DeWilde ¹⁴⁸,
 S. Dhaliwal ¹⁵⁸, R. Dhullipudi ^{24,m}, A. Di Ciaccio ^{133a,133b}, L. Di Ciaccio ⁴, A. Di Girolamo ²⁹,
 B. Di Girolamo ²⁹, S. Di Luise ^{134a,134b}, A. Di Mattia ¹⁷³, B. Di Micco ²⁹, R. Di Nardo ⁴⁷,
 A. Di Simone ^{133a,133b}, R. Di Sipio ^{19a,19b}, M.A. Diaz ^{31a}, F. Diblen ^{18c}, E.B. Diehl ⁸⁷, J. Dietrich ⁴¹,
 T.A. Dietzsch ^{58a}, S. Diglio ⁸⁶, K. Dindar Yagci ³⁹, J. Dingfelder ²⁰, C. Dionisi ^{132a,132b}, P. Dita ^{25a}, S. Dita ^{25a},
 F. Dittus ²⁹, F. Djama ⁸³, T. Djobava ^{51b}, M.A.B. do Vale ^{23c}, A. Do Valle Wemans ^{124a,n}, T.K.O. Doan ⁴,
 M. Dobbs ⁸⁵, R. Dobinson ^{29,*}, D. Dobos ²⁹, E. Dobson ^{29,o}, J. Dodd ³⁴, C. Doglioni ⁴⁹, T. Doherty ⁵³,
 Y. Doi ^{65,*}, J. Dolejsi ¹²⁶, I. Dolenc ⁷⁴, Z. Dolezal ¹²⁶, B.A. Dolgoshein ^{96,*}, T. Dohmae ¹⁵⁵, M. Donadelli ^{23d},
 M. Donega ¹²⁰, J. Donini ³³, J. Dopke ²⁹, A. Doria ^{102a}, A. Dos Anjos ¹⁷³, A. Dotti ^{122a,122b}, M.T. Dova ⁷⁰,
 A.D. Doxiadis ¹⁰⁵, A.T. Doyle ⁵³, M. Dris ⁹, J. Dubbert ⁹⁹, S. Dube ¹⁴, E. Duchovni ¹⁷², G. Duckeck ⁹⁸,
 A. Dudarev ²⁹, F. Dudziak ⁶³, M. Dührssen ²⁹, I.P. Duerdoth ⁸², L. Duflot ¹¹⁵, M.-A. Dufour ⁸⁵, M. Dunford ²⁹,
 H. Duran Yildiz ^{3a}, R. Duxfield ¹³⁹, M. Dwuznik ³⁷, F. Dydak ²⁹, M. Düren ⁵², J. Ebke ⁹⁸, S. Eckweiler ⁸¹,
 K. Edmonds ⁸¹, C.A. Edwards ⁷⁶, N.C. Edwards ⁵³, W. Ehrenfeld ⁴¹, T. Eifert ¹⁴³, G. Eigen ¹³, K. Einsweiler ¹⁴,
 E. Eisenhandler ⁷⁵, T. Ekelof ¹⁶⁶, M. El Kacimi ^{135c}, M. Ellert ¹⁶⁶, S. Elles ⁴, F. Ellinghaus ⁸¹, K. Ellis ⁷⁵,
 N. Ellis ²⁹, J. Elmsheuser ⁹⁸, M. Elsing ²⁹, D. Emeliyanov ¹²⁹, R. Engelmann ¹⁴⁸, A. Engl ⁹⁸, B. Epp ⁶¹,
 A. Eppig ⁸⁷, J. Erdmann ⁵⁴, A. Ereditato ¹⁶, D. Eriksson ^{146a}, J. Ernst ¹, M. Ernst ²⁴, J. Ernwein ¹³⁶,
 D. Errede ¹⁶⁵, S. Errede ¹⁶⁵, E. Ertel ⁸¹, M. Escalier ¹¹⁵, C. Escobar ¹²³, X. Espinal Curull ¹¹, B. Esposito ⁴⁷,
 F. Etienne ⁸³, A.I. Etienvre ¹³⁶, E. Etzion ¹⁵³, D. Evangelakou ⁵⁴, H. Evans ⁶⁰, L. Fabbri ^{19a,19b}, C. Fabre ²⁹,
 R.M. Fakhruddinov ¹²⁸, S. Falciano ^{132a}, Y. Fang ¹⁷³, M. Fanti ^{89a,89b}, A. Farbin ⁷, A. Farilla ^{134a}, J. Farley ¹⁴⁸,
 T. Farooque ¹⁵⁸, S. Farrell ¹⁶³, S.M. Farrington ¹¹⁸, P. Farthouat ²⁹, P. Fassnacht ²⁹, D. Fassouliotis ⁸,
 B. Fathollahzadeh ¹⁵⁸, A. Favareto ^{89a,89b}, L. Fayard ¹¹⁵, S. Fazio ^{36a,36b}, R. Febbraro ³³, P. Federic ^{144a},
 O.L. Fedin ¹²¹, W. Fedorko ⁸⁸, M. Fehling-Kaschek ⁴⁸, L. Feligioni ⁸³, D. Fellmann ⁵, C. Feng ^{32d}, E.J. Feng ³⁰,
 A.B. Fenyuk ¹²⁸, J. Ferencei ^{144b}, W. Fernando ⁵, S. Ferrag ⁵³, J. Ferrando ⁵³, V. Ferrara ⁴¹, A. Ferrari ¹⁶⁶,
 P. Ferrari ¹⁰⁵, R. Ferrari ^{119a}, D.E. Ferreira de Lima ⁵³, A. Ferrer ¹⁶⁷, D. Ferrere ⁴⁹, C. Ferretti ⁸⁷,
 A. Ferretto Parodi ^{50a,50b}, M. Fiascaris ³⁰, F. Fiedler ⁸¹, A. Filipčič ⁷⁴, F. Filthaut ¹⁰⁴, M. Fincke-Keeler ¹⁶⁹,
 M.C.N. Fiolhais ^{124a,h}, L. Fiorini ¹⁶⁷, A. Firan ³⁹, G. Fischer ⁴¹, M.J. Fisher ¹⁰⁹, M. Flechl ⁴⁸, I. Fleck ¹⁴¹,
 J. Fleckner ⁸¹, P. Fleischmann ¹⁷⁴, S. Fleischmann ¹⁷⁵, T. Flick ¹⁷⁵, A. Floderus ⁷⁹, L.R. Flores Castillo ¹⁷³,
 M.J. Flowerdew ⁹⁹, T. Fonseca Martin ¹⁶, A. Formica ¹³⁶, A. Forti ⁸², D. Fortin ^{159a}, D. Fournier ¹¹⁵, H. Fox ⁷¹,
 P. Francavilla ¹¹, S. Franchino ^{119a,119b}, D. Francis ²⁹, T. Frank ¹⁷², M. Franklin ⁵⁷, S. Franz ²⁹,
 M. Fraternali ^{119a,119b}, S. Fratina ¹²⁰, S.T. French ²⁷, C. Friedrich ⁴¹, F. Friedrich ⁴³, R. Froeschl ²⁹,
 D. Froidevaux ²⁹, J.A. Frost ²⁷, C. Fukunaga ¹⁵⁶, E. Fullana Torregrosa ²⁹, B.G. Fulsom ¹⁴³, J. Fuster ¹⁶⁷,
 C. Gabaldon ²⁹, O. Gabizon ¹⁷², T. Gadfort ²⁴, S. Gadomski ⁴⁹, G. Gagliardi ^{50a,50b}, P. Gagnon ⁶⁰, C. Galea ⁹⁸,
 E.J. Gallas ¹¹⁸, V. Gallo ¹⁶, B.J. Gallop ¹²⁹, P. Gallus ¹²⁵, K.K. Gan ¹⁰⁹, Y.S. Gao ^{143,e}, A. Gaponenko ¹⁴,
 F. Garberon ¹⁷⁶, M. Garcia-Sciveres ¹⁴, C. García ¹⁶⁷, J.E. García Navarro ¹⁶⁷, R.W. Gardner ³⁰, N. Garelli ²⁹,
 H. Garitaonandia ¹⁰⁵, V. Garonne ²⁹, J. Garvey ¹⁷, C. Gatti ⁴⁷, G. Gaudio ^{119a}, B. Gaur ¹⁴¹, L. Gauthier ¹³⁶,
 P. Gauzzi ^{132a,132b}, I.L. Gavrilenko ⁹⁴, C. Gay ¹⁶⁸, G. Gaycken ²⁰, E.N. Gazis ⁹, P. Ge ^{32d}, Z. Gece ¹⁶⁸,
 C.N.P. Gee ¹²⁹, D.A.A. Geerts ¹⁰⁵, Ch. Geich-Gimbel ²⁰, K. Gellerstedt ^{146a,146b}, C. Gemme ^{50a},
 A. Gemmell ⁵³, M.H. Genest ⁵⁵, S. Gentile ^{132a,132b}, M. George ⁵⁴, S. George ⁷⁶, P. Gerlach ¹⁷⁵,
 A. Gershon ¹⁵³, C. Geweniger ^{58a}, H. Ghazlane ^{135b}, N. Ghodbane ³³, B. Jacobbe ^{19a}, S. Giagu ^{132a,132b},
 V. Giakoumopoulou ⁸, V. Giangiobbe ¹¹, F. Gianotti ²⁹, B. Gibbard ²⁴, A. Gibson ¹⁵⁸, S.M. Gibson ²⁹,
 D. Gillberg ²⁸, A.R. Gillman ¹²⁹, D.M. Gingrich ^{2,d}, J. Ginzburg ¹⁵³, N. Giokaris ⁸, M.P. Giordani ^{164c},

R. Giordano^{102a,102b}, F.M. Giorgi¹⁵, P. Giovannini⁹⁹, P.F. Giraud¹³⁶, D. Giugni^{89a}, M. Giunta⁹³, P. Giusti^{19a}, B.K. Gjelsten¹¹⁷, L.K. Gladilin⁹⁷, C. Glasman⁸⁰, J. Glatzer⁴⁸, A. Glazov⁴¹, K.W. Glitza¹⁷⁵, G.L. Glonti⁶⁴, J.R. Goddard⁷⁵, J. Godfrey¹⁴², J. Godlewski²⁹, M. Goebel⁴¹, T. Göpfert⁴³, C. Goeringer⁸¹, C. Gössling⁴², T. Göttfert⁹⁹, S. Goldfarb⁸⁷, T. Golling¹⁷⁶, A. Gomes^{124a,b}, L.S. Gomez Fajardo⁴¹, R. Gonçalo⁷⁶, J. Goncalves Pinto Firmino Da Costa⁴¹, L. Gonella²⁰, S. Gonzalez¹⁷³, S. González de la Hoz¹⁶⁷, G. Gonzalez Parra¹¹, M.L. Gonzalez Silva²⁶, S. Gonzalez-Sevilla⁴⁹, J.J. Goodson¹⁴⁸, L. Goossens²⁹, P.A. Gorbounov⁹⁵, H.A. Gordon²⁴, I. Gorelov¹⁰³, G. Gorfine¹⁷⁵, B. Gorini²⁹, E. Gorini^{72a,72b}, A. Gorišek⁷⁴, E. Gornicki³⁸, B. Gosdzik⁴¹, A.T. Goshaw⁵, M. Gosselink¹⁰⁵, M.I. Gostkin⁶⁴, I. Gough Eschrich¹⁶³, M. Gouighri^{135a}, D. Goujdami^{135c}, M.P. Goulette⁴⁹, A.G. Goussiou¹³⁸, C. Goy⁴, S. Gozpinar²², I. Grabowska-Bold³⁷, P. Grafström²⁹, K.-J. Grah⁴¹, F. Grancagnolo^{72a}, S. Grancagnolo¹⁵, V. Grassi¹⁴⁸, V. Gratchev¹²¹, N. Grau³⁴, H.M. Gray²⁹, J.A. Gray¹⁴⁸, E. Graziani^{134a}, O.G. Grebenyuk¹²¹, T. Greenshaw⁷³, Z.D. Greenwood^{24,m}, K. Gregersen³⁵, I.M. Gregor⁴¹, P. Grenier¹⁴³, J. Griffiths¹³⁸, N. Grigalashvili⁶⁴, A.A. Grillo¹³⁷, S. Grinstein¹¹, Y.V. Grishkevich⁹⁷, J.-F. Grivaz¹¹⁵, E. Gross¹⁷², J. Grosse-Knetter⁵⁴, J. Groth-Jensen¹⁷², K. Grybel¹⁴¹, D. Guest¹⁷⁶, C. Guicheney³³, A. Guida^{72a,72b}, S. Guindon⁵⁴, H. Guler^{85,p}, J. Gunther¹²⁵, B. Guo¹⁵⁸, J. Guo³⁴, V.N. Gushchin¹²⁸, P. Gutierrez¹¹¹, N. Guttman¹⁵³, O. Gutzwiller¹⁷³, C. Guyot¹³⁶, C. Gwenlan¹¹⁸, C.B. Gwilliam⁷³, A. Haas¹⁴³, S. Haas²⁹, C. Haber¹⁴, H.K. Hadavand³⁹, D.R. Hadley¹⁷, P. Haefner⁹⁹, F. Hahn²⁹, S. Haider²⁹, Z. Hajduk³⁸, H. Hakobyan¹⁷⁷, D. Hall¹¹⁸, J. Haller⁵⁴, K. Hamacher¹⁷⁵, P. Hamal¹¹³, M. Hamer⁵⁴, A. Hamilton^{145b,q}, S. Hamilton¹⁶¹, L. Han^{32b}, K. Hanagaki¹¹⁶, K. Hanawa¹⁶⁰, M. Hance¹⁴, C. Handel⁸¹, P. Hanke^{58a}, J.R. Hansen³⁵, J.B. Hansen³⁵, J.D. Hansen³⁵, P.H. Hansen³⁵, P. Hansson¹⁴³, K. Hara¹⁶⁰, G.A. Hare¹³⁷, T. Harenberg¹⁷⁵, S. Harkusha⁹⁰, D. Harper⁸⁷, R.D. Harrington⁴⁵, O.M. Harris¹³⁸, K. Harrison¹⁷, J. Hartert⁴⁸, F. Hartjes¹⁰⁵, T. Haruyama⁶⁵, A. Harvey⁵⁶, S. Hasegawa¹⁰¹, Y. Hasegawa¹⁴⁰, S. Hassani¹³⁶, S. Haug¹⁶, M. Hauschild²⁹, R. Hauser⁸⁸, M. Havranek²⁰, C.M. Hawkes¹⁷, R.J. Hawkins²⁹, A.D. Hawkins⁷⁹, D. Hawkins¹⁶³, T. Hayakawa⁶⁶, T. Hayashi¹⁶⁰, D. Hayden⁷⁶, H.S. Hayward⁷³, S.J. Haywood¹²⁹, M. He^{32d}, S.J. Head¹⁷, V. Hedberg⁷⁹, L. Heelan⁷, S. Heim⁸⁸, B. Heinemann¹⁴, S. Heisterkamp³⁵, L. Helary⁴, C. Heller⁹⁸, M. Heller²⁹, S. Hellman^{146a,146b}, D. Hellmich²⁰, C. Helsens¹¹, R.C.W. Henderson⁷¹, M. Henke^{58a}, A. Henrichs⁵⁴, A.M. Henriques Correia²⁹, S. Henrot-Versille¹¹⁵, F. Henry-Couannier⁸³, C. Hensel⁵⁴, T. Henß¹⁷⁵, C.M. Hernandez⁷, Y. Hernández Jiménez¹⁶⁷, R. Herrberg¹⁵, G. Herten⁴⁸, R. Hertenberger⁹⁸, L. Hervas²⁹, G.G. Hesketh⁷⁷, N.P. Hessey¹⁰⁵, E. Higón-Rodríguez¹⁶⁷, J.C. Hill²⁷, K.H. Hiller⁴¹, S. Hillert²⁰, S.J. Hillier¹⁷, I. Hinchliffe¹⁴, E. Hines¹²⁰, M. Hirose¹¹⁶, F. Hirsch⁴², D. Hirschbuehl¹⁷⁵, J. Hobbs¹⁴⁸, N. Hod¹⁵³, M.C. Hodgkinson¹³⁹, P. Hodgson¹³⁹, A. Hoecker²⁹, M.R. Hoferkamp¹⁰³, J. Hoffman³⁹, D. Hoffmann⁸³, M. Hohlfeld⁸¹, M. Holder¹⁴¹, S.O. Holmgren^{146a}, T. Holy¹²⁷, J.L. Holzbauer⁸⁸, T.M. Hong¹²⁰, L. Hooft van Huysduynen¹⁰⁸, C. Horn¹⁴³, S. Horner⁴⁸, J.-Y. Hostachy⁵⁵, S. Hou¹⁵¹, A. Hoummada^{135a}, J. Howarth⁸², I. Hristova¹⁵, J. Hrivnac¹¹⁵, I. Hruska¹²⁵, T. Hryn'ova⁴, P.J. Hsu⁸¹, S.-C. Hsu¹⁴, Z. Hubacek¹²⁷, F. Hubaut⁸³, F. Huegging²⁰, A. Huettmann⁴¹, T.B. Huffman¹¹⁸, E.W. Hughes³⁴, G. Hughes⁷¹, M. Huhtinen²⁹, M. Hurwitz¹⁴, U. Husemann⁴¹, N. Huseynov^{64,r}, J. Huston⁸⁸, J. Huth⁵⁷, G. Iacobucci⁴⁹, G. Iakovidis⁹, M. Ibbotson⁸², I. Ibragimov¹⁴¹, L. Iconomidou-Fayard¹¹⁵, J. Idarraga¹¹⁵, P. Iengo^{102a}, O. Igonkina¹⁰⁵, Y. Ikegami⁶⁵, M. Ikeno⁶⁵, D. Iliadis¹⁵⁴, N. Ilic¹⁵⁸, T. Ince²⁰, J. Inigo-Golfín²⁹, P. Ioannou⁸, M. Iodice^{134a}, K. Iordanidou⁸, V. Ippolito^{132a,132b}, A. Irlés Quiles¹⁶⁷, C. Isaksson¹⁶⁶, A. Ishikawa⁶⁶, M. Ishino⁶⁷, R. Ishmukhametov³⁹, C. Issever¹¹⁸, S. Istin^{18a}, A.V. Ivashin¹²⁸, W. Iwanski³⁸, H. Iwasaki⁶⁵, J.M. Izen⁴⁰, V. Izzo^{102a}, B. Jackson¹²⁰, J.N. Jackson⁷³, P. Jackson¹⁴³, M.R. Jaekel²⁹, V. Jain⁶⁰, K. Jakobs⁴⁸, S. Jakobsen³⁵, J. Jakubek¹²⁷, D.K. Jana¹¹¹, E. Jansen⁷⁷, H. Jansen²⁹, A. Jantsch⁹⁹, M. Janus⁴⁸, G. Jarlskog⁷⁹, L. Jeanty⁵⁷, I. Jen-La Plante³⁰, P. Jenni²⁹, A. Jeremie⁴, P. Jež³⁵, S. Jézéquel⁴, M.K. Jha^{19a}, H. Ji¹⁷³, W. Ji⁸¹, J. Jia¹⁴⁸, Y. Jiang^{32b}, M. Jimenez Belenguer⁴¹, S. Jin^{32a}, O. Jinnouchi¹⁵⁷, M.D. Joergensen³⁵, D. Joffe³⁹, L.G. Johansen¹³, M. Johansen^{146a,146b}, K.E. Johansson^{146a}, P. Johansson¹³⁹, S. Johnert⁴¹, K.A. Johns⁶, K. Jon-And^{146a,146b}, G. Jones¹¹⁸, R.W.L. Jones⁷¹, T.J. Jones⁷³, C. Joram²⁹, P.M. Jorge^{124a}, K.D. Joshi⁸², J. Jovicevic¹⁴⁷, T. Jovin^{12b}, X. Ju¹⁷³, C.A. Jung⁴², R.M. Jungst²⁹, V. Juranek¹²⁵, P. Jussel⁶¹, A. Juste Rozas¹¹, S. Kabana¹⁶, M. Kaci¹⁶⁷, A. Kaczmarska³⁸, P. Kadlecik³⁵, M. Kado¹¹⁵, H. Kagan¹⁰⁹, M. Kagan⁵⁷, E. Kajomovitz¹⁵², S. Kalinin¹⁷⁵, L.V. Kalinovskaya⁶⁴, S. Kama³⁹, N. Kanaya¹⁵⁵, M. Kaneda²⁹, S. Kaneti²⁷, T. Kanno¹⁵⁷, V.A. Kantserov⁹⁶, J. Kanzaki⁶⁵, B. Kaplan¹⁷⁶, A. Kapliy³⁰, J. Kaplon²⁹, D. Kar⁵³,

M. Karagounis²⁰, K. Karakostas⁹, M. Karnevskiy⁴¹, V. Kartvelishvili⁷¹, A.N. Karyukhin¹²⁸, L. Kashif¹⁷³,
 G. Kasieczka^{58b}, R.D. Kass¹⁰⁹, A. Kastanas¹³, M. Kataoka⁴, Y. Kataoka¹⁵⁵, E. Katsoufis⁹, J. Katzy⁴¹,
 V. Kaushik⁶, K. Kawagoe⁶⁹, T. Kawamoto¹⁵⁵, G. Kawamura⁸¹, M.S. Kayl¹⁰⁵, V.A. Kazanin¹⁰⁷,
 M.Y. Kazarinov⁶⁴, R. Keeler¹⁶⁹, R. Kehoe³⁹, M. Keil⁵⁴, G.D. Kekelidze⁶⁴, J.S. Keller¹³⁸, J. Kennedy⁹⁸,
 M. Kenyon⁵³, O. Kepka¹²⁵, N. Kerschen²⁹, B.P. Kerševan⁷⁴, S. Kersten¹⁷⁵, K. Kessoku¹⁵⁵, J. Keung¹⁵⁸,
 F. Khalil-zada¹⁰, H. Khandanyan¹⁶⁵, A. Khanov¹¹², D. Kharchenko⁶⁴, A. Khodinov⁹⁶, A. Khomich^{58a},
 T.J. Khoo²⁷, G. Khorauli²⁰, A. Khoroshilov¹⁷⁵, V. Khovanskiy⁹⁵, E. Khramov⁶⁴, J. Khubua^{51b},
 H. Kim^{146a,146b}, M.S. Kim², S.H. Kim¹⁶⁰, N. Kimura¹⁷¹, O. Kind¹⁵, B.T. King⁷³, M. King⁶⁶, R.S.B. King¹¹⁸,
 J. Kirk¹²⁹, A.E. Kiryunin⁹⁹, T. Kishimoto⁶⁶, D. Kisielewska³⁷, T. Kittelmann¹²³, A.M. Kiver¹²⁸,
 E. Kladiva^{144b}, M. Klein⁷³, U. Klein⁷³, K. Kleinknecht⁸¹, M. Klemetti⁸⁵, A. Klier¹⁷², P. Klimek^{146a,146b},
 A. Klimentov²⁴, R. Klingenberg⁴², J.A. Klinger⁸², E.B. Klinkby³⁵, T. Klioutchnikova²⁹, P.F. Klok¹⁰⁴,
 S. Klous¹⁰⁵, E.-E. Kluge^{58a}, T. Kluge⁷³, P. Kluit¹⁰⁵, S. Kluth⁹⁹, N.S. Knecht¹⁵⁸, E. Kneringer⁶¹,
 E.B.F.G. Knoop⁸³, A. Knue⁵⁴, B.R. Ko⁴⁴, T. Kobayashi¹⁵⁵, M. Kobel⁴³, M. Kocian¹⁴³, P. Kodys¹²⁶,
 K. Köneke²⁹, A.C. König¹⁰⁴, S. Koenig⁸¹, L. Köpke⁸¹, F. Koetsveld¹⁰⁴, P. Koevesarki²⁰, T. Koffas²⁸,
 E. Koffeman¹⁰⁵, L.A. Kogan¹¹⁸, S. Kohlmann¹⁷⁵, F. Kohn⁵⁴, Z. Kohout¹²⁷, T. Kohriki⁶⁵, T. Koi¹⁴³,
 G.M. Kolachev¹⁰⁷, H. Kolanoski¹⁵, V. Kolesnikov⁶⁴, I. Koletsou^{89a}, J. Koll⁸⁸, M. Kollfrath⁴⁸,
 A.A. Komar⁹⁴, Y. Komori¹⁵⁵, T. Kondo⁶⁵, T. Kono^{41,s}, A.I. Kononov⁴⁸, R. Konoplich^{108,t},
 N. Konstantinidis⁷⁷, A. Kootz¹⁷⁵, S. Koperny³⁷, K. Korcyl³⁸, K. Kordas¹⁵⁴, A. Korn¹¹⁸, A. Korol¹⁰⁷,
 I. Korolkov¹¹, E.V. Korolkova¹³⁹, V.A. Korotkov¹²⁸, O. Kortner⁹⁹, S. Kortner⁹⁹, V.V. Kostyukhin²⁰,
 S. Kotov⁹⁹, V.M. Kotov⁶⁴, A. Kotwal⁴⁴, C. Kourkoumelis⁸, V. Kouskoura¹⁵⁴, A. Koutsman^{159a},
 R. Kowalewski¹⁶⁹, T.Z. Kowalski³⁷, W. Kozanecki¹³⁶, A.S. Kozhin¹²⁸, V. Kral¹²⁷, V.A. Kramarenko⁹⁷,
 G. Kramberger⁷⁴, M.W. Krasny⁷⁸, A. Krasznahorkay¹⁰⁸, J. Kraus⁸⁸, J.K. Kraus²⁰, F. Krejci¹²⁷,
 J. Kretzschmar⁷³, N. Krieger⁵⁴, P. Krieger¹⁵⁸, K. Kroeninger⁵⁴, H. Kroha⁹⁹, J. Kroll¹²⁰, J. Kroseberg²⁰,
 J. Krstic^{12a}, U. Kruchonak⁶⁴, H. Krüger²⁰, T. Kruker¹⁶, N. Krumnack⁶³, Z.V. Krumshteyn⁶⁴, A. Kruth²⁰,
 T. Kubota⁸⁶, S. Kudah^{3a}, S. Kuehn⁴⁸, A. Kugel^{58c}, T. Kuhl⁴¹, D. Kuhn⁶¹, V. Kukhtin⁶⁴, Y. Kulchitsky⁹⁰,
 S. Kuleshov^{31b}, C. Kummer⁹⁸, M. Kuna⁷⁸, J. Kunkle¹²⁰, A. Kupco¹²⁵, H. Kurashige⁶⁶, M. Kurata¹⁶⁰,
 Y.A. Kurochkin⁹⁰, V. Kus¹²⁵, E.S. Kuwertz¹⁴⁷, M. Kuze¹⁵⁷, J. Kvita¹⁴², R. Kwee¹⁵, A. La Rosa⁴⁹,
 L. La Rotonda^{36a,36b}, L. Labarga⁸⁰, J. Labbe⁴, S. Lablak^{135a}, C. Lacasta¹⁶⁷, F. Lacava^{132a,132b}, H. Lacker¹⁵,
 D. Lacour⁷⁸, V.R. Lacuesta¹⁶⁷, E. Ladygin⁶⁴, R. Lafaye⁴, B. Laforge⁷⁸, T. Lagouri⁸⁰, S. Lai⁴⁸, E. Laisne⁵⁵,
 M. Lamanna²⁹, L. Lambourne⁷⁷, C.L. Lampen⁶, W. Lampl⁶, E. Lancon¹³⁶, U. Landgraf⁴⁸, M.P.J. Landon⁷⁵,
 J.L. Lane⁸², C. Lange⁴¹, A.J. Lankford¹⁶³, F. Lanni²⁴, K. Lantsch¹⁷⁵, S. Laplace⁷⁸, C. Lapoire²⁰,
 J.F. Laporte¹³⁶, T. Lari^{89a}, A. Larner¹¹⁸, M. Lassnig²⁹, P. Laurelli⁴⁷, V. Lavorini^{36a,36b}, W. Lavrijsen¹⁴,
 P. Laycock⁷³, O. Le Dortz⁷⁸, E. Le Guirriec⁸³, C. Le Maner¹⁵⁸, E. Le Menedeu¹¹, T. LeCompte⁵,
 F. Ledroit-Guillon⁵⁵, H. Lee¹⁰⁵, J.S.H. Lee¹¹⁶, S.C. Lee¹⁵¹, L. Lee¹⁷⁶, M. Lefebvre¹⁶⁹, M. Legendre¹³⁶,
 B.C. LeGeyt¹²⁰, F. Legger⁹⁸, C. Leggett¹⁴, M. Lehmacher²⁰, G. Lehmann Miotto²⁹, X. Lei⁶,
 M.A.L. Leite^{23d}, R. Leitner¹²⁶, D. Lellouch¹⁷², B. Lemmer⁵⁴, V. Lendermann^{58a}, K.J.C. Leney^{145b},
 T. Lenz¹⁰⁵, G. Lenzen¹⁷⁵, B. Lenzi²⁹, K. Leonhardt⁴³, S. Leontsinis⁹, F. Lepold^{58a}, C. Leroy⁹³,
 J.-R. Lessard¹⁶⁹, C.G. Lester²⁷, C.M. Lester¹²⁰, J. Levêque⁴, D. Levin⁸⁷, L.J. Levinson¹⁷², A. Lewis¹¹⁸,
 G.H. Lewis¹⁰⁸, A.M. Leyko²⁰, M. Leyton¹⁵, B. Li⁸³, H. Li^{173,u}, S. Li^{32b,v}, X. Li⁸⁷, Z. Liang^{118,w}, H. Liao³³,
 B. Liberti^{133a}, P. Lichard²⁹, M. Lichtnecker⁹⁸, K. Lie¹⁶⁵, W. Liebig¹³, C. Limbach²⁰, A. Limosani⁸⁶,
 M. Limper⁶², S.C. Lin^{151,x}, F. Linde¹⁰⁵, J.T. Linnemann⁸⁸, E. Lipeles¹²⁰, A. Lipniacka¹³, T.M. Liss¹⁶⁵,
 D. Lissauer²⁴, A. Lister⁴⁹, A.M. Litke¹³⁷, C. Liu²⁸, D. Liu¹⁵¹, H. Liu⁸⁷, J.B. Liu⁸⁷, M. Liu^{32b}, Y. Liu^{32b},
 M. Livan^{119a,119b}, S.S.A. Livermore¹¹⁸, A. Lleres⁵⁵, J. Llorente Merino⁸⁰, S.L. Lloyd⁷⁵, E. Lobodzinska⁴¹,
 P. Loch⁶, W.S. Lockman¹³⁷, T. Loddenkoetter²⁰, F.K. Loebinger⁸², A. Loginov¹⁷⁶, C.W. Loh¹⁶⁸, T. Lohse¹⁵,
 K. Lohwasser⁴⁸, M. Lokajicek¹²⁵, V.P. Lombardo⁴, R.E. Long⁷¹, L. Lopes^{124a}, D. Lopez Mateos⁵⁷,
 J. Lorenz⁹⁸, N. Lorenzo Martinez¹¹⁵, M. Losada¹⁶², P. Loscutoff¹⁴, F. Lo Sterzo^{132a,132b}, M.J. Losty^{159a},
 X. Lou⁴⁰, A. Lounis¹¹⁵, K.F. Loureiro¹⁶², J. Love²¹, P.A. Love⁷¹, A.J. Lowe^{143,e}, F. Lu^{32a}, H.J. Lubatti¹³⁸,
 C. Luci^{132a,132b}, A. Lucotte⁵⁵, A. Ludwig⁴³, D. Ludwig⁴¹, I. Ludwig⁴⁸, J. Ludwig⁴⁸, F. Luehring⁶⁰,
 G. Luijckx¹⁰⁵, W. Lukas⁶¹, D. Lumb⁴⁸, L. Luminari^{132a}, E. Lund¹¹⁷, B. Lund-Jensen¹⁴⁷, B. Lundberg⁷⁹,
 J. Lundberg^{146a,146b}, J. Lundquist³⁵, M. Lungwitz⁸¹, D. Lynn²⁴, J. Lys¹⁴, E. Lytken⁷⁹, H. Ma²⁴, L.L. Ma¹⁷³,
 J.A. Macana Goia⁹³, G. Maccarrone⁴⁷, A. Macchiolo⁹⁹, B. Maček⁷⁴, J. Machado Miguens^{124a},
 R. Mackeprang³⁵, R.J. Madaras¹⁴, W.F. Mader⁴³, R. Maenner^{58c}, T. Maeno²⁴, P. Mättig¹⁷⁵, S. Mättig⁴¹,

L. Magnoni²⁹, E. Magradze⁵⁴, K. Mahboubi⁴⁸, S. Mahmoud⁷³, G. Mahout¹⁷, C. Maiani^{132a,132b},
 C. Maidantchik^{23a}, A. Maio^{124a,b}, S. Majewski²⁴, Y. Makida⁶⁵, N. Makovec¹¹⁵, P. Mal¹³⁶, B. Malaescu²⁹,
 Pa. Malecki³⁸, P. Malecki³⁸, V.P. Maleev¹²¹, F. Malek⁵⁵, U. Mallik⁶², D. Malon⁵, C. Malone¹⁴³,
 S. Maltezos⁹, V. Malyshev¹⁰⁷, S. Malyukov²⁹, R. Mameghani⁹⁸, J. Mamuzic^{12b}, A. Manabe⁶⁵,
 L. Mandelli^{89a}, I. Mandić⁷⁴, R. Mandrysch¹⁵, J. Maneira^{124a}, P.S. Mangedard⁸⁸,
 L. Manhaes de Andrade Filho^{23a}, A. Mann⁵⁴, P.M. Manning¹³⁷, A. Manousakis-Katsikakis⁸,
 B. Mansoulie¹³⁶, A. Mapelli²⁹, L. Mapelli²⁹, L. March⁸⁰, J.F. Marchand²⁸, F. Marchese^{133a,133b},
 G. Marchiori⁷⁸, M. Marcisovsky¹²⁵, C.P. Marino¹⁶⁹, F. Marroquim^{23a}, Z. Marshall²⁹, F.K. Martens¹⁵⁸,
 S. Marti-Garcia¹⁶⁷, B. Martin²⁹, B. Martin⁸⁸, J.P. Martin⁹³, T.A. Martin¹⁷, V.J. Martin⁴⁵,
 B. Martin dit Latour⁴⁹, S. Martin-Haugh¹⁴⁹, M. Martinez¹¹, V. Martinez Outschoorn⁵⁷,
 A.C. Martyniuk¹⁶⁹, M. Marx⁸², F. Marzano^{132a}, A. Marzin¹¹¹, L. Masetti⁸¹, T. Mashimo¹⁵⁵,
 R. Mashinistov⁹⁴, J. Masik⁸², A.L. Maslennikov¹⁰⁷, I. Massa^{19a,19b}, G. Massaro¹⁰⁵, N. Massol⁴,
 P. Mastrandrea^{132a,132b}, A. Mastroberardino^{36a,36b}, T. Masubuchi¹⁵⁵, P. Matricon¹¹⁵, H. Matsunaga¹⁵⁵,
 T. Matsushita⁶⁶, C. Mattravers^{118,c}, J. Maurer⁸³, S.J. Maxfield⁷³, A. Mayne¹³⁹, R. Mazini¹⁵¹, M. Mazur²⁰,
 L. Mazzaferro^{133a,133b}, M. Mazzanti^{89a}, S.P. Mc Kee⁸⁷, A. McCarn¹⁶⁵, R.L. McCarthy¹⁴⁸, T.G. McCarthy²⁸,
 N.A. McCubbin¹²⁹, K.W. McFarlane⁵⁶, J.A. McFayden¹³⁹, H. McGlone⁵³, G. Mchedlidze^{51b},
 T. McLaughlan¹⁷, S.J. McMahon¹²⁹, R.A. McPherson^{169,k}, A. Meade⁸⁴, J. Mechnich¹⁰⁵, M. Mechtel¹⁷⁵,
 M. Medinnis⁴¹, R. Meera-Lebbai¹¹¹, T. Meguro¹¹⁶, R. Mehdiev⁹³, S. Mehlhase³⁵, A. Mehta⁷³,
 K. Meier^{58a}, B. Meirose⁷⁹, C. Melachrinou³⁰, B.R. Mellado Garcia¹⁷³, F. Meloni^{89a,89b},
 L. Mendoza Navas¹⁶², Z. Meng^{151,u}, A. Mengarelli^{19a,19b}, S. Menke⁹⁹, E. Meoni¹¹, K.M. Mercurio⁵⁷,
 P. Mermod⁴⁹, L. Merola^{102a,102b}, C. Meroni^{89a}, F.S. Merritt³⁰, H. Merritt¹⁰⁹, A. Messina^{29,y},
 J. Metcalfe¹⁰³, A.S. Mete⁶³, C. Meyer⁸¹, C. Meyer³⁰, J.-P. Meyer¹³⁶, J. Meyer¹⁷⁴, J. Meyer⁵⁴,
 T.C. Meyer²⁹, W.T. Meyer⁶³, J. Miao^{32d}, S. Michal²⁹, L. Micu^{25a}, R.P. Middleton¹²⁹, S. Migas⁷³,
 L. Mijović⁴¹, G. Mikenberg¹⁷², M. Mikestikova¹²⁵, M. Mikuž⁷⁴, D.W. Miller³⁰, R.J. Miller⁸⁸,
 W.J. Mills¹⁶⁸, C. Mills⁵⁷, A. Milov¹⁷², D.A. Milstead^{146a,146b}, D. Milstein¹⁷², A.A. Minaenko¹²⁸,
 M. Miñano Moya¹⁶⁷, I.A. Minashvili⁶⁴, A.I. Mincer¹⁰⁸, B. Mindur³⁷, M. Mineev⁶⁴, Y. Ming¹⁷³,
 L.M. Mir¹¹, G. Mirabelli^{132a}, A. Misiejuk⁷⁶, J. Mitrevski¹³⁷, V.A. Mitsou¹⁶⁷, S. Mitsui⁶⁵,
 P.S. Miyagawa¹³⁹, K. Miyazaki⁶⁶, J.U. Mjörnmark⁷⁹, T. Moa^{146a,146b}, S. Moed⁵⁷, V. Moeller²⁷,
 K. Mönig⁴¹, N. Möser²⁰, S. Mohapatra¹⁴⁸, W. Mohr⁴⁸, R. Moles-Valls¹⁶⁷, J. Molina-Perez²⁹, J. Monk⁷⁷,
 E. Monnier⁸³, S. Montesano^{89a,89b}, F. Monticelli⁷⁰, S. Monzani^{19a,19b}, R.W. Moore², G.F. Moorhead⁸⁶,
 C. Mora Herrera⁴⁹, A. Moraes⁵³, N. Morange¹³⁶, J. Morel⁵⁴, G. Morello^{36a,36b}, D. Moreno⁸¹,
 M. Moreno Llácer¹⁶⁷, P. Morettini^{50a}, M. Morgenstern⁴³, M. Morii⁵⁷, J. Morin⁷⁵, A.K. Morley²⁹,
 G. Mornacchi²⁹, J.D. Morris⁷⁵, L. Morvaj¹⁰¹, H.G. Moser⁹⁹, M. Mosidze^{51b}, J. Moss¹⁰⁹, R. Mount¹⁴³,
 E. Mountricha^{9,z}, S.V. Mouraviev⁹⁴, E.J.W. Moyses⁸⁴, F. Mueller^{58a}, J. Mueller¹²³, K. Mueller²⁰,
 T.A. Müller⁹⁸, T. Mueller⁸¹, D. Muenstermann²⁹, Y. Munwes¹⁵³, W.J. Murray¹²⁹, I. Mussche¹⁰⁵,
 E. Musto^{102a,102b}, A.G. Myagkov¹²⁸, M. Myska¹²⁵, J. Nadal¹¹, K. Nagai¹⁶⁰, K. Nagano⁶⁵, A. Nagarkar¹⁰⁹,
 Y. Nagasaka⁵⁹, M. Nagel⁹⁹, A.M. Nairz²⁹, Y. Nakahama²⁹, K. Nakamura¹⁵⁵, T. Nakamura¹⁵⁵,
 I. Nakano¹¹⁰, G. Nanava²⁰, A. Napier¹⁶¹, R. Narayan^{58b}, M. Nash^{77,c}, T. Nattermann²⁰, T. Naumann⁴¹,
 G. Navarro¹⁶², H.A. Neal⁸⁷, P.Yu. Nechaeva⁹⁴, T.J. Neep⁸², A. Negri^{119a,119b}, G. Negri²⁹, S. Nektarijevic⁴⁹,
 A. Nelson¹⁶³, T.K. Nelson¹⁴³, S. Nemecek¹²⁵, P. Nemethy¹⁰⁸, A.A. Nepomuceno^{23a}, M. Nessi^{29,aa},
 M.S. Neubauer¹⁶⁵, A. Neusiedl⁸¹, R.M. Neves¹⁰⁸, P. Nevski²⁴, P.R. Newman¹⁷, V. Nguyen Thi Hong¹³⁶,
 R.B. Nickerson¹¹⁸, R. Nicolaidou¹³⁶, L. Nicolas¹³⁹, B. Nicquevert²⁹, F. Niedercorn¹¹⁵, J. Nielsen¹³⁷,
 N. Nikiforou³⁴, A. Nikiforov¹⁵, V. Nikolaenko¹²⁸, I. Nikolic-Audit⁷⁸, K. Nikolics⁴⁹, K. Nikolopoulos²⁴,
 H. Nilsen⁴⁸, P. Nilsson⁷, Y. Ninomiya¹⁵⁵, A. Nisati^{132a}, T. Nishiyama⁶⁶, R. Nisius⁹⁹, L. Nodulman⁵,
 M. Nomachi¹¹⁶, I. Nomidis¹⁵⁴, M. Nordberg²⁹, P.R. Norton¹²⁹, J. Novakova¹²⁶, M. Nozaki⁶⁵, L. Nozka¹¹³,
 I.M. Nugent^{159a}, A.-E. Nuncio-Quiroz²⁰, G. Nunes Hanninger⁸⁶, T. Nunnemann⁹⁸, E. Nurse⁷⁷,
 B.J. O'Brien⁴⁵, S.W. O'Neale^{17,*}, D.C. O'Neil¹⁴², V. O'Shea⁵³, L.B. Oakes⁹⁸, F.G. Oakham^{28,d},
 H. Oberlack⁹⁹, J. Ocariz⁷⁸, A. Ochi⁶⁶, S. Oda¹⁵⁵, S. Odaka⁶⁵, J. Odier⁸³, H. Ogren⁶⁰, A. Oh⁸², S.H. Oh⁴⁴,
 C.C. Ohm^{146a,146b}, T. Ohshima¹⁰¹, S. Okada⁶⁶, H. Okawa¹⁶³, Y. Okumura¹⁰¹, T. Okuyama¹⁵⁵,
 A. Olariu^{25a}, A.G. Olchevski⁶⁴, S.A. Olivares Pino^{31a}, M. Oliveira^{124a,h}, D. Oliveira Damazio²⁴,
 E. Oliver Garcia¹⁶⁷, D. Olivito¹²⁰, A. Olszewski³⁸, J. Olszowska³⁸, A. Onofre^{124a,ab}, P.U.E. Onyisi³⁰,
 C.J. Oram^{159a}, M.J. Oreglia³⁰, Y. Oren¹⁵³, D. Orestano^{134a,134b}, N. Orlando^{72a,72b}, I. Orlov¹⁰⁷,

C. Oropeza Barrera⁵³, R.S. Orr¹⁵⁸, B. Osculati^{50a,50b}, R. Ospanov¹²⁰, C. Osuna¹¹, G. Otero y Garzon²⁶, J.P. Ottersbach¹⁰⁵, M. Ouchrif^{135d}, E.A. Ouellette¹⁶⁹, F. Ould-Saada¹¹⁷, A. Ouraou¹³⁶, Q. Ouyang^{32a}, A. Ovcharova¹⁴, M. Owen⁸², S. Owen¹³⁹, V.E. Ozcan^{18a}, N. Ozturk⁷, A. Pacheco Pages¹¹, C. Padilla Aranda¹¹, S. Pagan Griso¹⁴, E. Paganis¹³⁹, F. Paige²⁴, P. Pais⁸⁴, K. Pajchel¹¹⁷, G. Palacino^{159b}, C.P. Paleari⁶, S. Palestini²⁹, D. Pallin³³, A. Palma^{124a}, J.D. Palmer¹⁷, Y.B. Pan¹⁷³, E. Panagiotopoulou⁹, N. Panikashvili⁸⁷, S. Panitkin²⁴, D. Pantea^{25a}, A. Papadelis^{146a}, Th.D. Papadopoulou⁹, A. Paramonov⁵, D. Paredes Hernandez³³, W. Park^{24,ac}, M.A. Parker²⁷, F. Parodi^{50a,50b}, J.A. Parsons³⁴, U. Parzefall⁴⁸, S. Pashapour⁵⁴, E. Pasqualucci^{132a}, S. Passaggio^{50a}, A. Passeri^{134a}, F. Pastore^{134a,134b}, Fr. Pastore⁷⁶, G. Pásztor^{49,ad}, S. Pataraja¹⁷⁵, N. Patel¹⁵⁰, J.R. Pater⁸², S. Patricelli^{102a,102b}, T. Pauly²⁹, M. Pecsny^{144a}, M.I. Pedraza Morales¹⁷³, S.V. Peleganchuk¹⁰⁷, D. Pelikan¹⁶⁶, H. Peng^{32b}, B. Penning³⁰, A. Penson³⁴, J. Penwell⁶⁰, M. Perantoni^{23a}, K. Perez^{34,ae}, T. Perez Cavalcanti⁴¹, E. Perez Codina^{159a}, M.T. Pérez García-Estañ¹⁶⁷, V. Perez Reale³⁴, L. Perini^{89a,89b}, H. Pernegger²⁹, R. Perrino^{72a}, P. Perrodo⁴, S. Persema^{3a}, V.D. Peshekhonov⁶⁴, K. Peters²⁹, B.A. Petersen²⁹, J. Petersen²⁹, T.C. Petersen³⁵, E. Petit⁴, A. Petridis¹⁵⁴, C. Petridou¹⁵⁴, E. Petrolu^{132a}, F. Petrucci^{134a,134b}, D. Petschull⁴¹, M. Petteni¹⁴², R. Pezoa^{31b}, A. Phan⁸⁶, P.W. Phillips¹²⁹, G. Piacquadio²⁹, A. Picazio⁴⁹, E. Piccaro⁷⁵, M. Piccinini^{19a,19b}, S.M. Piec⁴¹, R. Piegai²⁶, D.T. Pignotti¹⁰⁹, J.E. Pilcher³⁰, A.D. Pilkington⁸², J. Pina^{124a,b}, M. Pinamonti^{164a,164c}, A. Pinder¹¹⁸, J.L. Pinfold², B. Pinto^{124a}, C. Pizio^{89a,89b}, M. Plamondon¹⁶⁹, M.-A. Pleier²⁴, E. Plotnikova⁶⁴, A. Poblaguev²⁴, S. Poddar^{58a}, F. Podlyski³³, L. Poggioli¹¹⁵, T. Poghosyan²⁰, M. Pohl⁴⁹, F. Polci⁵⁵, G. Polesello^{119a}, A. Policicchio^{36a,36b}, A. Polini^{19a}, J. Poll⁷⁵, V. Polychronakos²⁴, D.M. Pomarede¹³⁶, D. Pomeroy²², K. Pommès²⁹, L. Pontecorvo^{132a}, B.G. Pope⁸⁸, G.A. Popeneciu^{25a}, D.S. Popovic^{12a}, A. Poppleton²⁹, X. Portell Bueso²⁹, G.E. Pospelov⁹⁹, S. Pospisil¹²⁷, I.N. Potrap⁹⁹, C.J. Potter¹⁴⁹, C.T. Potter¹¹⁴, G. Poulard²⁹, J. Poveda¹⁷³, V. Pozdnyakov⁶⁴, R. Prabhu⁷⁷, P. Pralavorio⁸³, A. Pranko¹⁴, S. Prasad²⁹, R. Pravahan²⁴, S. Prell⁶³, K. Pretzl¹⁶, D. Price⁶⁰, J. Price⁷³, L.E. Price⁵, D. Prieur¹²³, M. Primavera^{72a}, K. Prokofiev¹⁰⁸, F. Prokoshin^{31b}, S. Protopopescu²⁴, J. Proudfoot⁵, X. Prudent⁴³, M. Przybycien³⁷, H. Przysiezniak⁴, S. Psoroulas²⁰, E. Ptacek¹¹⁴, E. Pueschel⁸⁴, J. Purdham⁸⁷, M. Purohit^{24,ac}, P. Puze¹¹⁵, Y. Pylypchenko⁶², J. Qian⁸⁷, Z. Qin⁴¹, A. Quadt⁵⁴, D.R. Quarrie¹⁴, W.B. Quayle¹⁷³, F. Quinonez^{31a}, M. Raas¹⁰⁴, V. Radescu⁴¹, P. Radloff¹¹⁴, T. Rador^{18a}, F. Ragusa^{89a,89b}, G. Rahal¹⁷⁸, A.M. Rahimi¹⁰⁹, D. Rahm²⁴, S. Rajagopalan²⁴, M. Rammensee⁴⁸, M. Rammes¹⁴¹, A.S. Randle-Conde³⁹, K. Randrianarivony²⁸, F. Rauscher⁹⁸, T.C. Rave⁴⁸, M. Raymond²⁹, A.L. Read¹¹⁷, D.M. Rebuszi^{119a,119b}, A. Redelbach¹⁷⁴, G. Redlinger²⁴, R. Reece¹²⁰, K. Reeves⁴⁰, E. Reinherz-Aronis¹⁵³, A. Reinsch¹¹⁴, I. Reisinger⁴², C. Rembser²⁹, Z.L. Ren¹⁵¹, A. Renaud¹¹⁵, M. Rescigno^{132a}, S. Resconi^{89a}, B. Resende¹³⁶, P. Reznicek⁹⁸, R. Rezvani¹⁵⁸, R. Richter⁹⁹, E. Richter-Was^{4,af}, M. Ridel⁷⁸, M. Rijpstra¹⁰⁵, M. Rijssenbeek¹⁴⁸, A. Rimoldi^{119a,119b}, L. Rinaldi^{19a}, R.R. Rios³⁹, I. Riu¹¹, G. Rivoltella^{89a,89b}, F. Rizatdinova¹¹², E. Rizvi⁷⁵, S.H. Robertson^{85,k}, A. Robichaud-Veronneau¹¹⁸, D. Robinson²⁷, J.E.M. Robinson⁷⁷, A. Robson⁵³, J.G. Rocha de Lima¹⁰⁶, C. Roda^{122a,122b}, D. Roda Dos Santos²⁹, A. Roe⁵⁴, S. Roe²⁹, O. Røhne¹¹⁷, S. Rolli¹⁶¹, A. Romaniouk⁹⁶, M. Romano^{19a,19b}, G. Romeo²⁶, E. Romero Adam¹⁶⁷, L. Roos⁷⁸, E. Ros¹⁶⁷, S. Rosati^{132a}, K. Rosbach⁴⁹, A. Rose¹⁴⁹, M. Rose⁷⁶, G.A. Rosenbaum¹⁵⁸, E.I. Rosenberg⁶³, P.L. Rosendahl¹³, O. Rosenthal¹⁴¹, L. Rosselet⁴⁹, V. Rossetti¹¹, E. Rossi^{132a,132b}, L.P. Rossi^{50a}, M. Rotaru^{25a}, I. Roth¹⁷², J. Rothberg¹³⁸, D. Rousseau¹¹⁵, C.R. Royon¹³⁶, A. Rozanov⁸³, Y. Rozen¹⁵², X. Ruan^{32a,ag}, F. Rubbo¹¹, I. Rubinskiy⁴¹, B. Ruckert⁹⁸, N. Ruckstuhl¹⁰⁵, V.I. Rud⁹⁷, C. Rudolph⁴³, G. Rudolph⁶¹, F. Rühr⁶, F. Ruggieri^{134a,134b}, A. Ruiz-Martinez⁶³, L. Rummyantsev⁶⁴, K. Runge⁴⁸, Z. Rurikova⁴⁸, N.A. Rusakovich⁶⁴, J.P. Rutherford⁶, C. Ruwiedel¹⁴, P. Ruzicka¹²⁵, Y.F. Ryabov¹²¹, P. Ryan⁸⁸, M. Rybar¹²⁶, G. Rybkin¹¹⁵, N.C. Ryder¹¹⁸, A.F. Saavedra¹⁵⁰, I. Sadeh¹⁵³, H.F.-W. Sadrozinski¹³⁷, R. Sadykov⁶⁴, F. Safai Tehrani^{132a}, H. Sakamoto¹⁵⁵, G. Salamanna⁷⁵, A. Salamon^{133a}, M. Saleem¹¹¹, D. Salek²⁹, D. Salihagic⁹⁹, A. Salnikov¹⁴³, J. Salt¹⁶⁷, B.M. Salvachua Ferrando⁵, D. Salvatore^{36a,36b}, F. Salvatore¹⁴⁹, A. Salvucci¹⁰⁴, A. Salzburger²⁹, D. Sampsonidis¹⁵⁴, B.H. Samset¹¹⁷, A. Sanchez^{102a,102b}, V. Sanchez Martinez¹⁶⁷, H. Sandaker¹³, H.G. Sander⁸¹, M.P. Sanders⁹⁸, M. Sandhoff¹⁷⁵, T. Sandoval²⁷, C. Sandoval¹⁶², R. Sandstroem⁹⁹, D.P.C. Sankey¹²⁹, A. Sansoni⁴⁷, C. Santamarina Rios⁸⁵, C. Santoni³³, R. Santonico^{133a,133b}, H. Santos^{124a}, J.G. Saraiva^{124a}, T. Sarangi¹⁷³, E. Sarkisyan-Grinbaum⁷, F. Sarri^{122a,122b}, G. Sartisohn¹⁷⁵, O. Sasaki⁶⁵, N. Sasao⁶⁷, I. Satsounkevitch⁹⁰, G. Sauvage⁴, E. Sauvan⁴, J.B. Sauvan¹¹⁵, P. Savard^{158,d}, V. Savinov¹²³, D.O. Savu²⁹, L. Sawyer^{24,m}, D.H. Saxon⁵³, J. Saxon¹²⁰, C. Sbarra^{19a}, A. Sbrizzi^{19a,19b}, O. Scallion⁹³,

D.A. Scannicchio¹⁶³, M. Scarcella¹⁵⁰, J. Schaarschmidt¹¹⁵, P. Schacht⁹⁹, D. Schaefer¹²⁰, U. Schäfer⁸¹,
 S. Schaepe²⁰, S. Schaezel^{58b}, A.C. Schaffer¹¹⁵, D. Schaile⁹⁸, R.D. Schamberger¹⁴⁸, A.G. Schamov¹⁰⁷,
 V. Scharf^{58a}, V.A. Schegelsky¹²¹, D. Scheirich⁸⁷, M. Schernau¹⁶³, M.I. Scherzer³⁴, C. Schiavi^{50a,50b},
 J. Schieck⁹⁸, M. Schioppa^{36a,36b}, S. Schlenker²⁹, E. Schmidt⁴⁸, K. Schmieden²⁰, C. Schmitt⁸¹,
 S. Schmitt^{58b}, M. Schmitz²⁰, A. Schöning^{58b}, M. Schott²⁹, D. Schouten^{159a}, J. Schovancova¹²⁵,
 M. Schram⁸⁵, C. Schroeder⁸¹, N. Schroer^{58c}, M.J. Schultens²⁰, J. Schultes¹⁷⁵, H.-C. Schultz-Coulon^{58a},
 H. Schulz¹⁵, J.W. Schumacher²⁰, M. Schumacher⁴⁸, B.A. Schumm¹³⁷, Ph. Schune¹³⁶,
 C. Schwanenberger⁸², A. Schwartzman¹⁴³, Ph. Schwemling⁷⁸, R. Schwienhorst⁸⁸, R. Schwierz⁴³,
 J. Schwindling¹³⁶, T. Schwindt²⁰, M. Schwoerer⁴, G. Sciolla²², W.G. Scott¹²⁹, J. Searcy¹¹⁴, G. Sedov⁴¹,
 E. Sedykh¹²¹, S.C. Seidel¹⁰³, A. Seiden¹³⁷, F. Seifert⁴³, J.M. Seixas^{23a}, G. Sekhniaidze^{102a},
 S.J. Sekula³⁹, K.E. Selbach⁴⁵, D.M. Seliverstov¹²¹, B. Sellden^{146a}, G. Sellers⁷³, M. Seman^{144b},
 N. Semprini-Cesari^{19a,19b}, C. Serfon⁹⁸, L. Serin¹¹⁵, L. Serkin⁵⁴, R. Seuster⁹⁹, H. Severini¹¹¹, A. Sfyrla²⁹,
 E. Shabalina⁵⁴, M. Shamim¹¹⁴, L.Y. Shan^{32a}, J.T. Shank²¹, Q.T. Shao⁸⁶, M. Shapiro¹⁴, P.B. Shatalov⁹⁵,
 K. Shaw^{164a,164c}, D. Sherman¹⁷⁶, P. Sherwood⁷⁷, A. Shibata¹⁰⁸, H. Shichi¹⁰¹, S. Shimizu²⁹,
 M. Shimojima¹⁰⁰, T. Shin⁵⁶, M. Shiyakova⁶⁴, A. Shmeleva⁹⁴, M.J. Shochet³⁰, D. Short¹¹⁸, S. Shrestha⁶³,
 E. Shulga⁹⁶, M.A. Shupe⁶, P. Sicho¹²⁵, A. Sidoti^{132a}, F. Siegert⁴⁸, Dj. Sijacki^{12a}, O. Silbert¹⁷², J. Silva^{124a},
 Y. Silver¹⁵³, D. Silverstein¹⁴³, S.B. Silverstein^{146a}, V. Simak¹²⁷, O. Simard¹³⁶, Lj. Simic^{12a}, S. Simion¹¹⁵,
 B. Simmons⁷⁷, R. Simoniello^{89a,89b}, M. Simonyan³⁵, P. Sinervo¹⁵⁸, N.B. Sinev¹¹⁴, V. Sipica¹⁴¹,
 G. Siragusa¹⁷⁴, A. Sircar²⁴, A.N. Sisakyan⁶⁴, S.Yu. Sivoklokov⁹⁷, J. Sjölin^{146a,146b}, T.B. Sjørnsen¹³,
 L.A. Skinnari¹⁴, H.P. Skottowe⁵⁷, K. Skovpen¹⁰⁷, P. Skubic¹¹¹, M. Slater¹⁷, T. Slavicek¹²⁷, K. Sliwa¹⁶¹,
 V. Smakhtin¹⁷², B.H. Smart⁴⁵, S.Yu. Smirnov⁹⁶, Y. Smirnov⁹⁶, L.N. Smirnova⁹⁷, O. Smirnova⁷⁹,
 B.C. Smith⁵⁷, D. Smith¹⁴³, K.M. Smith⁵³, M. Smizanska⁷¹, K. Smolek¹²⁷, A.A. Snesev⁹⁴, S.W. Snow⁸²,
 J. Snow¹¹¹, S. Snyder²⁴, R. Sobie^{169,k}, J. Sodomka¹²⁷, A. Soffer¹⁵³, C.A. Solans¹⁶⁷, M. Solar¹²⁷, J. Solc¹²⁷,
 E. Soldatov⁹⁶, U. Soldevila¹⁶⁷, E. Solfaroli Camillocci^{132a,132b}, A.A. Solodkov¹²⁸, O.V. Solovyanov¹²⁸,
 N. Soni², V. Sopko¹²⁷, B. Sopko¹²⁷, M. Sosebee⁷, R. Soualah^{164a,164c}, A. Soukharev¹⁰⁷,
 S. Spagnolo^{72a,72b}, F. Spanò⁷⁶, R. Spighi^{19a}, G. Spigo²⁹, F. Spila^{132a,132b}, R. Spiwoks²⁹, M. Spousta¹²⁶,
 T. Spreitzer¹⁵⁸, B. Spurlock⁷, R.D. St. Denis⁵³, J. Stahlman¹²⁰, R. Stamen^{58a}, E. Stanecka³⁸, R.W. Stanek⁵,
 C. Stanescu^{134a}, M. Stanescu-Bellu⁴¹, S. Stapnes¹¹⁷, E.A. Starchenko¹²⁸, J. Stark⁵⁵, P. Staroba¹²⁵,
 P. Starovoitov⁴¹, A. Staude⁹⁸, P. Stavina^{144a}, G. Steele⁵³, P. Steinbach⁴³, P. Steinberg²⁴, I. Stekl¹²⁷,
 B. Stelzer¹⁴², H.J. Stelzer⁸⁸, O. Stelzer-Chilton^{159a}, H. Stenzel⁵², S. Stern⁹⁹, G.A. Stewart²⁹,
 J.A. Stillings²⁰, M.C. Stockton⁸⁵, K. Stoerig⁴⁸, G. Stoicea^{25a}, S. Stonjek⁹⁹, P. Strachota¹²⁶, A.R. Stradling⁷,
 A. Straessner⁴³, J. Strandberg¹⁴⁷, S. Strandberg^{146a,146b}, A. Strandlie¹¹⁷, M. Strang¹⁰⁹, E. Strauss¹⁴³,
 M. Strauss¹¹¹, P. Strizenec^{144b}, R. Ströhmer¹⁷⁴, D.M. Strom¹¹⁴, J.A. Strong^{76,*}, R. Stroynowski³⁹,
 J. Strube¹²⁹, B. Stugu¹³, I. Stumer^{24,*}, J. Stupak¹⁴⁸, P. Sturm¹⁷⁵, N.A. Styles⁴¹, D.A. Soh^{151,w}, D. Su¹⁴³,
 HS. Subramania², A. Succurro¹¹, Y. Sugaya¹¹⁶, C. Suhr¹⁰⁶, K. Suita⁶⁶, M. Suk¹²⁶, V.V. Sulina⁹⁴,
 S. Sultansoy^{3d}, T. Sumida⁶⁷, X. Sun⁵⁵, J.E. Sundermann⁴⁸, K. Suruliz¹³⁹, G. Susinno^{36a,36b},
 M.R. Sutton¹⁴⁹, Y. Suzuki⁶⁵, Y. Suzuki⁶⁶, M. Svatos¹²⁵, S. Swedish¹⁶⁸, I. Sykora^{144a}, T. Sykora¹²⁶,
 J. Sánchez¹⁶⁷, D. Ta¹⁰⁵, K. Tackmann⁴¹, A. Taffard¹⁶³, R. Tahirout^{159a}, N. Taiblum¹⁵³, Y. Takahashi¹⁰¹,
 H. Takai²⁴, R. Takashima⁶⁸, H. Takeda⁶⁶, T. Takeshita¹⁴⁰, Y. Takubo⁶⁵, M. Talby⁸³, A. Talyshev^{107,f},
 M.C. Tamsett²⁴, J. Tanaka¹⁵⁵, R. Tanaka¹¹⁵, S. Tanaka¹³¹, S. Tanaka⁶⁵, A.J. Tanasijczuk¹⁴², K. Tani⁶⁶,
 N. Tannoury⁸³, S. Tapprogge⁸¹, D. Tardif¹⁵⁸, S. Tarem¹⁵², F. Tarrade²⁸, G.F. Tartarelli^{89a}, P. Tas¹²⁶,
 M. Tasevsky¹²⁵, E. Tassi^{36a,36b}, M. Tatarkhanov¹⁴, Y. Tayalati^{135d}, C. Taylor⁷⁷, F.E. Taylor⁹²,
 G.N. Taylor⁸⁶, W. Taylor^{159b}, M. Teinturier¹¹⁵, M. Teixeira Dias Castanheira⁷⁵, P. Teixeira-Dias⁷⁶,
 K.K. Temming⁴⁸, H. Ten Kate²⁹, P.K. Teng¹⁵¹, S. Terada⁶⁵, K. Terashi¹⁵⁵, J. Terron⁸⁰, M. Testa⁴⁷,
 R.J. Teuscher^{158,k}, J. Therhaag²⁰, T. Theveneaux-Pelzer⁷⁸, M. Thioye¹⁷⁶, S. Thoma⁴⁸, J.P. Thomas¹⁷,
 E.N. Thompson³⁴, P.D. Thompson¹⁷, P.D. Thompson¹⁵⁸, A.S. Thompson⁵³, L.A. Thomsen³⁵,
 E. Thomson¹²⁰, M. Thomson²⁷, R.P. Thun⁸⁷, F. Tian³⁴, M.J. Tibbetts¹⁴, T. Tic¹²⁵, V.O. Tikhomirov⁹⁴,
 Y.A. Tikhonov^{107,f}, S. Timoshenko⁹⁶, P. Tipton¹⁷⁶, F.J. Tique Aires Viegas²⁹, S. Tisserant⁸³, T. Todorov⁴,
 S. Todorova-Nova¹⁶¹, B. Toggerson¹⁶³, J. Tojo⁶⁹, S. Tokár^{144a}, K. Tokunaga⁶⁶, K. Tokushuku⁶⁵,
 K. Tollefson⁸⁸, M. Tomoto¹⁰¹, L. Tompkins³⁰, K. Toms¹⁰³, A. Tonoyan¹³, C. Topfel¹⁶, N.D. Topilin⁶⁴,
 I. Torchiani²⁹, E. Torrence¹¹⁴, H. Torres⁷⁸, E. Torró Pastor¹⁶⁷, J. Toth^{83,ad}, F. Touchard⁸³, D.R. Tovey¹³⁹,
 T. Trefzger¹⁷⁴, L. Tremblet²⁹, A. Tricoli²⁹, I.M. Trigger^{159a}, S. Trincaz-Duvold⁷⁸, M.F. Tripiana⁷⁰,

W. Trischuk¹⁵⁸, B. Trocmé⁵⁵, C. Troncon^{89a}, M. Trottier-McDonald¹⁴², M. Trzebinski³⁸, A. Trzupek³⁸,
 C. Tsarouchas²⁹, J.C.-L. Tseng¹¹⁸, M. Tsiakiris¹⁰⁵, P.V. Tsiarehka⁹⁰, D. Tsiou^{4,ah}, G. Tsipolitis⁹,
 V. Tsiskaridze⁴⁸, E.G. Tskhadadze^{51a}, I.I. Tsukerman⁹⁵, V. Tsulaia¹⁴, J.-W. Tsung²⁰, S. Tsuno⁶⁵,
 D. Tsybychev¹⁴⁸, A. Tua¹³⁹, A. Tudorache^{25a}, V. Tudorache^{25a}, J.M. Tuggle³⁰, M. Turala³⁸, D. Turecek¹²⁷,
 I. Turk Cakir^{3e}, E. Turlay¹⁰⁵, R. Turra^{89a,89b}, P.M. Tuts³⁴, A. Tykhonov⁷⁴, M. Tylmad^{146a,146b},
 M. Tyndel¹²⁹, G. Tzanakos⁸, K. Uchida²⁰, I. Ueda¹⁵⁵, R. Ueno²⁸, M. Ugland¹³, M. Uhlenbrock²⁰,
 M. Uhrmacher⁵⁴, F. Ukegawa¹⁶⁰, G. Unal²⁹, A. Undrus²⁴, G. Unel¹⁶³, Y. Unno⁶⁵, D. Urbaniec³⁴,
 G. Usai⁷, M. Uslenghi^{119a,119b}, L. Vacavant⁸³, V. Vacek¹²⁷, B. Vachon⁸⁵, S. Vahsen¹⁴, J. Valenta¹²⁵,
 P. Valente^{132a}, S. Valentinetti^{19a,19b}, S. Valkar¹²⁶, E. Valladolid Gallego¹⁶⁷, S. Vallecorsa¹⁵²,
 J.A. Valls Ferrer¹⁶⁷, H. van der Graaf¹⁰⁵, E. van der Kraaij¹⁰⁵, R. Van Der Leeuw¹⁰⁵, E. van der Poel¹⁰⁵,
 D. van der Ster²⁹, N. van Eldik²⁹, P. van Gemmeren⁵, I. van Vulpen¹⁰⁵, M. Vanadia⁹⁹, W. Vandelli²⁹,
 A. Vaniachine⁵, P. Vankov⁴¹, F. Vannucci⁷⁸, R. Vari^{132a}, T. Varol⁸⁴, D. Varouchas¹⁴, A. Vartapetian⁷,
 K.E. Varvell¹⁵⁰, V.I. Vassilakopoulos⁵⁶, F. Vazeille³³, T. Vazquez Schroeder⁵⁴, G. Vegni^{89a,89b},
 J.J. Veillet¹¹⁵, F. Veloso^{124a}, R. Veness²⁹, S. Veneziano^{132a}, A. Ventura^{72a,72b}, D. Ventura⁸⁴,
 M. Venturi⁴⁸, N. Venturi¹⁵⁸, V. Vercesi^{119a}, M. Verducci¹³⁸, W. Verkerke¹⁰⁵, J.C. Vermeulen¹⁰⁵,
 A. Vest⁴³, M.C. Vetterli^{142,d}, I. Vichou¹⁶⁵, T. Vickey^{145b,ai}, O.E. Vickey Boeriu^{145b}, G.H.A. Viehhauser¹¹⁸,
 S. Viel¹⁶⁸, M. Villa^{19a,19b}, M. Villaplana Perez¹⁶⁷, E. Vilucchi⁴⁷, M.G. Vincker²⁸, E. Vinek²⁹,
 V.B. Vinogradov⁶⁴, M. Virchaux^{136,*}, J. Virzi¹⁴, O. Vitells¹⁷², M. Viti⁴¹, I. Vivarelli⁴⁸, F. Vives Vaque²,
 S. Vlachos⁹, D. Vladoiu⁹⁸, M. Vlasak¹²⁷, A. Vogel²⁰, P. Vokac¹²⁷, G. Volpi⁴⁷, M. Volpi⁸⁶, G. Volpini^{89a},
 H. von der Schmitt⁹⁹, J. von Loeben⁹⁹, H. von Radziewski⁴⁸, E. von Toerne²⁰, V. Vorobel¹²⁶,
 V. Vorwerk¹¹, M. Vos¹⁶⁷, R. Voss²⁹, T.T. Voss¹⁷⁵, J.H. Vosseveld⁷³, N. Vranjes¹³⁶,
 M. Vranjes Milosavljevic¹⁰⁵, V. Vrba¹²⁵, M. Vreeswijk¹⁰⁵, T. Vu Anh⁴⁸, R. Vuillermet²⁹, I. Vukotic¹¹⁵,
 W. Wagner¹⁷⁵, P. Wagner¹²⁰, H. Wahlen¹⁷⁵, S. Wahrmund⁴³, J. Wakabayashi¹⁰¹, S. Walch⁸⁷,
 J. Walder⁷¹, R. Walker⁹⁸, W. Walkowiak¹⁴¹, R. Wall¹⁷⁶, P. Waller⁷³, C. Wang⁴⁴, H. Wang¹⁷³,
 H. Wang^{32b,aj}, J. Wang¹⁵¹, J. Wang⁵⁵, R. Wang¹⁰³, S.M. Wang¹⁵¹, T. Wang²⁰, A. Warburton⁸⁵,
 C.P. Ward²⁷, M. Warsinsky⁴⁸, A. Washbrook⁴⁵, C. Wasicki⁴¹, P.M. Watkins¹⁷, A.T. Watson¹⁷,
 I.J. Watson¹⁵⁰, M.F. Watson¹⁷, G. Watts¹³⁸, S. Watts⁸², A.T. Waugh¹⁵⁰, B.M. Waugh⁷⁷, M. Weber¹²⁹,
 M.S. Weber¹⁶, P. Weber⁵⁴, A.R. Weidberg¹¹⁸, P. Weigell⁹⁹, J. Weingarten⁵⁴, C. Weiser⁴⁸,
 H. Wellenstein²², P.S. Wells²⁹, T. Wenaus²⁴, D. Wendland¹⁵, Z. Weng^{151,w}, T. Wengler²⁹, S. Wenig²⁹,
 N. Wermes²⁰, M. Werner⁴⁸, P. Werner²⁹, M. Werth¹⁶³, M. Wessels^{58a}, J. Wetter¹⁶¹, C. Weydert⁵⁵,
 K. Whalen²⁸, S.J. Wheeler-Ellis¹⁶³, A. White⁷, M.J. White⁸⁶, S. White^{122a,122b}, S.R. Whitehead¹¹⁸,
 D. Whiteson¹⁶³, D. Whittington⁶⁰, F. Wicek¹¹⁵, D. Wicke¹⁷⁵, F.J. Wickens¹²⁹, W. Wiedenmann¹⁷³,
 M. Wielers¹²⁹, P. Wienemann²⁰, C. Wiglesworth⁷⁵, L.A.M. Wiik-Fuchs⁴⁸, P.A. Wijeratne⁷⁷,
 A. Wildauer¹⁶⁷, M.A. Wildt^{41,s}, I. Wilhelm¹²⁶, H.G. Wilkens²⁹, J.Z. Will⁹⁸, E. Williams³⁴,
 H.H. Williams¹²⁰, W. Willis³⁴, S. Willocq⁸⁴, J.A. Wilson¹⁷, M.G. Wilson¹⁴³, A. Wilson⁸⁷,
 I. Wingerter-Seez⁴, S. Winkelmann⁴⁸, F. Winklmeier²⁹, M. Wittgen¹⁴³, M.W. Wolter³⁸, H. Wolters^{124a,h},
 W.C. Wong⁴⁰, G. Wooden⁸⁷, B.K. Wosiek³⁸, J. Wotschack²⁹, M.J. Woudstra⁸², K.W. Wozniak³⁸,
 K. Wraight⁵³, C. Wright⁵³, M. Wright⁵³, B. Wrona⁷³, S.L. Wu¹⁷³, X. Wu⁴⁹, Y. Wu^{32b,ak}, E. Wulf³⁴,
 B.M. Wynne⁴⁵, S. Xella³⁵, M. Xiao¹³⁶, S. Xie⁴⁸, C. Xu^{32b,z}, D. Xu¹³⁹, B. Yabsley¹⁵⁰, S. Yacoob^{145b},
 M. Yamada⁶⁵, H. Yamaguchi¹⁵⁵, A. Yamamoto⁶⁵, K. Yamamoto⁶³, S. Yamamoto¹⁵⁵, T. Yamamura¹⁵⁵,
 T. Yamanaka¹⁵⁵, J. Yamaoka⁴⁴, T. Yamazaki¹⁵⁵, Y. Yamazaki⁶⁶, Z. Yan²¹, H. Yang⁸⁷, U.K. Yang⁸²,
 Y. Yang⁶⁰, Z. Yang^{146a,146b}, S. Yanush⁹¹, L. Yao^{32a}, Y. Yao¹⁴, Y. Yasu⁶⁵, G.V. Ybeles Smit¹³⁰, J. Ye³⁹,
 S. Ye²⁴, M. Yilmaz^{3c}, R. Yoosoofmiya¹²³, K. Yorita¹⁷¹, R. Yoshida⁵, C. Young¹⁴³, C.J. Young¹¹⁸,
 S. Youssef²¹, D. Yu²⁴, J. Yu⁷, J. Yu¹¹², L. Yuan⁶⁶, A. Yurkewicz¹⁰⁶, B. Zabinski³⁸, R. Zaidan⁶²,
 A.M. Zaitsev¹²⁸, Z. Zajacova²⁹, L. Zanello^{132a,132b}, A. Zaytsev¹⁰⁷, C. Zeitnitz¹⁷⁵, M. Zeman¹²⁵,
 A. Zemla³⁸, C. Zender²⁰, O. Zenin¹²⁸, T. Ženiš^{144a}, Z. Zinonos^{122a,122b}, S. Zenz¹⁴, D. Zerwas¹¹⁵,
 G. Zevi della Porta⁵⁷, Z. Zhan^{32d}, D. Zhang^{32b,aj}, H. Zhang⁸⁸, J. Zhang⁵, X. Zhang^{32d}, Z. Zhang¹¹⁵,
 L. Zhao¹⁰⁸, T. Zhao¹³⁸, Z. Zhao^{32b}, A. Zhemchugov⁶⁴, J. Zhong¹¹⁸, B. Zhou⁸⁷, N. Zhou¹⁶³, Y. Zhou¹⁵¹,
 C.G. Zhu^{32d}, H. Zhu⁴¹, J. Zhu⁸⁷, Y. Zhu^{32b}, X. Zhuang⁹⁸, V. Zhuravlov⁹⁹, D. Zieminska⁶⁰,
 R. Zimmermann²⁰, S. Zimmermann²⁰, S. Zimmermann⁴⁸, M. Ziolkowski¹⁴¹, R. Zitoun⁴,
 L. Živković³⁴, V.V. Zmouchko^{128,*}, G. Zobernig¹⁷³, A. Zoccoli^{19a,19b}, M. zur Nedden¹⁵,
 V. Zutshi¹⁰⁶, L. Zwalinski²⁹

- ¹ University at Albany, Albany, NY, United States
- ² Department of Physics, University of Alberta, Edmonton, AB, Canada
- ³ ^(a) Department of Physics, Ankara University, Ankara; ^(b) Department of Physics, Dumlupinar University, Kutahya; ^(c) Department of Physics, Gazi University, Ankara; ^(d) Division of Physics, TOBB University of Economics and Technology, Ankara; ^(e) Turkish Atomic Energy Authority, Ankara, Turkey
- ⁴ LAPP, CNRS/IN2P3 and Université de Savoie, Annecy-le-Vieux, France
- ⁵ High Energy Physics Division, Argonne National Laboratory, Argonne, IL, United States
- ⁶ Department of Physics, University of Arizona, Tucson, AZ, United States
- ⁷ Department of Physics, The University of Texas at Arlington, Arlington, TX, United States
- ⁸ Physics Department, University of Athens, Athens, Greece
- ⁹ Physics Department, National Technical University of Athens, Zografou, Greece
- ¹⁰ Institute of Physics, Azerbaijan Academy of Sciences, Baku, Azerbaijan
- ¹¹ Institut de Física d'Altes Energies and Departament de Física de la Universitat Autònoma de Barcelona and ICREA, Barcelona, Spain
- ¹² ^(a) Institute of Physics, University of Belgrade, Belgrade; ^(b) Vinca Institute of Nuclear Sciences, University of Belgrade, Belgrade, Serbia
- ¹³ Department for Physics and Technology, University of Bergen, Bergen, Norway
- ¹⁴ Physics Division, Lawrence Berkeley National Laboratory and University of California, Berkeley, CA, United States
- ¹⁵ Department of Physics, Humboldt University, Berlin, Germany
- ¹⁶ Albert Einstein Center for Fundamental Physics and Laboratory for High Energy Physics, University of Bern, Bern, Switzerland
- ¹⁷ School of Physics and Astronomy, University of Birmingham, Birmingham, United Kingdom
- ¹⁸ ^(a) Department of Physics, Bogazici University, Istanbul; ^(b) Division of Physics, Dogus University, Istanbul; ^(c) Department of Physics Engineering, Gaziantep University, Gaziantep; ^(d) Department of Physics, Istanbul Technical University, Istanbul, Turkey
- ¹⁹ ^(a) INFN Sezione di Bologna; ^(b) Dipartimento di Fisica, Università di Bologna, Bologna, Italy
- ²⁰ Physikalisches Institut, University of Bonn, Bonn, Germany
- ²¹ Department of Physics, Boston University, Boston, MA, United States
- ²² Department of Physics, Brandeis University, Waltham, MA, United States
- ²³ ^(a) Universidade Federal do Rio De Janeiro COPPE/EE/IF, Rio de Janeiro; ^(b) Federal University of Juiz de Fora (UFJF), Juiz de Fora; ^(c) Federal University of Sao Joao del Rei (UFSJ), Sao Joao del Rei; ^(d) Instituto de Física, Universidade de Sao Paulo, Sao Paulo, Brazil
- ²⁴ Physics Department, Brookhaven National Laboratory, Upton, NY, United States
- ²⁵ ^(a) National Institute of Physics and Nuclear Engineering, Bucharest; ^(b) University Politehnica Bucharest, Bucharest; ^(c) West University in Timisoara, Timisoara, Romania
- ²⁶ Departamento de Física, Universidad de Buenos Aires, Buenos Aires, Argentina
- ²⁷ Cavendish Laboratory, University of Cambridge, Cambridge, United Kingdom
- ²⁸ Department of Physics, Carleton University, Ottawa, ON, Canada
- ²⁹ CERN, Geneva, Switzerland
- ³⁰ Enrico Fermi Institute, University of Chicago, Chicago, IL, United States
- ³¹ ^(a) Departamento de Física, Pontificia Universidad Católica de Chile, Santiago; ^(b) Departamento de Física, Universidad Técnica Federico Santa María, Valparaíso, Chile
- ³² ^(a) Institute of High Energy Physics, Chinese Academy of Sciences, Beijing; ^(b) Department of Modern Physics, University of Science and Technology of China, Anhui; ^(c) Department of Physics, Nanjing University, Jiangsu; ^(d) School of Physics, Shandong University, Shandong, China
- ³³ Laboratoire de Physique Corpusculaire, Clermont Université and Université Blaise Pascal and CNRS/IN2P3, Aubiere Cedex, France
- ³⁴ Nevis Laboratory, Columbia University, Irvington, NY, United States
- ³⁵ Niels Bohr Institute, University of Copenhagen, Copenhagen, Denmark
- ³⁶ ^(a) INFN Gruppo Collegato di Cosenza; ^(b) Dipartimento di Fisica, Università della Calabria, Arcavacata di Rende, Italy
- ³⁷ AGH University of Science and Technology, Faculty of Physics and Applied Computer Science, Krakow, Poland
- ³⁸ The Henryk Niewodniczanski Institute of Nuclear Physics, Polish Academy of Sciences, Krakow, Poland
- ³⁹ Physics Department, Southern Methodist University, Dallas, TX, United States
- ⁴⁰ Physics Department, University of Texas at Dallas, Richardson, TX, United States
- ⁴¹ DESY, Hamburg and Zeuthen, Germany
- ⁴² Institut für Experimentelle Physik IV, Technische Universität Dortmund, Dortmund, Germany
- ⁴³ Institut für Kern- und Teilchenphysik, Technical University Dresden, Dresden, Germany
- ⁴⁴ Department of Physics, Duke University, Durham, NC, United States
- ⁴⁵ SUPA – School of Physics and Astronomy, University of Edinburgh, Edinburgh, United Kingdom
- ⁴⁶ Fachhochschule Wiener Neustadt, Johannes Gutenbergstrasse 3 2700 Wiener Neustadt, Austria
- ⁴⁷ INFN Laboratori Nazionali di Frascati, Frascati, Italy
- ⁴⁸ Fakultät für Mathematik und Physik, Albert-Ludwigs-Universität, Freiburg i.Br., Germany
- ⁴⁹ Section de Physique, Université de Genève, Geneva, Switzerland
- ⁵⁰ ^(a) INFN Sezione di Genova; ^(b) Dipartimento di Fisica, Università di Genova, Genova, Italy
- ⁵¹ ^(a) E. Andronikashvili Institute of Physics, Tbilisi State University, Tbilisi; ^(b) High Energy Physics Institute, Tbilisi State University, Tbilisi, Georgia
- ⁵² II Physikalisches Institut, Justus-Liebig-Universität Giessen, Giessen, Germany
- ⁵³ SUPA – School of Physics and Astronomy, University of Glasgow, Glasgow, United Kingdom
- ⁵⁴ II Physikalisches Institut, Georg-August-Universität, Göttingen, Germany
- ⁵⁵ Laboratoire de Physique Subatomique et de Cosmologie, Université Joseph Fourier and CNRS/IN2P3 and Institut National Polytechnique de Grenoble, Grenoble, France
- ⁵⁶ Department of Physics, Hampton University, Hampton, VA, United States
- ⁵⁷ Laboratory for Particle Physics and Cosmology, Harvard University, Cambridge, MA, United States
- ⁵⁸ ^(a) Kirchhoff-Institut für Physik, Ruprecht-Karls-Universität Heidelberg, Heidelberg; ^(b) Physikalisches Institut, Ruprecht-Karls-Universität Heidelberg, Heidelberg;
- ⁵⁹ ZITI Institut für technische Informatik, Ruprecht-Karls-Universität Heidelberg, Mannheim, Germany
- ⁶⁰ Faculty of Applied Information Science, Hiroshima Institute of Technology, Hiroshima, Japan
- ⁶¹ Department of Physics, Indiana University, Bloomington, IN, United States
- ⁶² Institut für Astro- und Teilchenphysik, Leopold-Franzens-Universität, Innsbruck, Austria
- ⁶³ University of Iowa, Iowa City, IA, United States
- ⁶⁴ Department of Physics and Astronomy, Iowa State University, Ames, IA, United States
- ⁶⁵ Joint Institute for Nuclear Research, JINR Dubna, Dubna, Russia
- ⁶⁶ KEK, High Energy Accelerator Research Organization, Tsukuba, Japan
- ⁶⁷ Graduate School of Science, Kobe University, Kobe, Japan
- ⁶⁸ Faculty of Science, Kyoto University, Kyoto, Japan
- ⁶⁹ Kyoto University of Education, Kyoto, Japan
- ⁷⁰ Department of Physics, Kyushu University, Fukuoka, Japan
- ⁷¹ Instituto de Física La Plata, Universidad Nacional de La Plata and CONICET, La Plata, Argentina
- ⁷² Physics Department, Lancaster University, Lancaster, United Kingdom
- ⁷³ ^(a) INFN Sezione di Lecce; ^(b) Dipartimento di Matematica e Fisica, Università del Salento, Lecce, Italy
- ⁷⁴ Oliver Lodge Laboratory, University of Liverpool, Liverpool, United Kingdom
- ⁷⁵ Department of Physics, Jožef Stefan Institute and University of Ljubljana, Ljubljana, Slovenia

- ⁷⁵ School of Physics and Astronomy, Queen Mary University of London, London, United Kingdom
- ⁷⁶ Department of Physics, Royal Holloway University of London, Surrey, United Kingdom
- ⁷⁷ Department of Physics and Astronomy, University College London, London, United Kingdom
- ⁷⁸ Laboratoire de Physique Nucléaire et de Hautes Energies, UPMC and Université Paris-Diderot and CNRS/IN2P3, Paris, France
- ⁷⁹ Fysiska Institutionen, Lunds Universitet, Lund, Sweden
- ⁸⁰ Departamento de Física Teórica C-15, Universidad Autónoma de Madrid, Madrid, Spain
- ⁸¹ Institut für Physik, Universität Mainz, Mainz, Germany
- ⁸² School of Physics and Astronomy, University of Manchester, Manchester, United Kingdom
- ⁸³ CPPM, Aix-Marseille Université and CNRS/IN2P3, Marseille, France
- ⁸⁴ Department of Physics, University of Massachusetts, Amherst, MA, United States
- ⁸⁵ Department of Physics, McGill University, Montreal, QC, Canada
- ⁸⁶ School of Physics, University of Melbourne, Victoria, Australia
- ⁸⁷ Department of Physics, The University of Michigan, Ann Arbor, MI, United States
- ⁸⁸ Department of Physics and Astronomy, Michigan State University, East Lansing, MI, United States
- ⁸⁹ ^(a) INFN Sezione di Milano; ^(b) Dipartimento di Fisica, Università di Milano, Milano, Italy
- ⁹⁰ B.I. Stepanov Institute of Physics, National Academy of Sciences of Belarus, Minsk, Belarus
- ⁹¹ National Scientific and Educational Centre for Particle and High Energy Physics, Minsk, Belarus
- ⁹² Department of Physics, Massachusetts Institute of Technology, Cambridge, MA, United States
- ⁹³ Group of Particle Physics, University of Montreal, Montreal, QC, Canada
- ⁹⁴ P.N. Lebedev Institute of Physics, Academy of Sciences, Moscow, Russia
- ⁹⁵ Institute for Theoretical and Experimental Physics (ITEP), Moscow, Russia
- ⁹⁶ Moscow Engineering and Physics Institute (MEPhI), Moscow, Russia
- ⁹⁷ Skobeltsyn Institute of Nuclear Physics, Lomonosov Moscow State University, Moscow, Russia
- ⁹⁸ Fakultät für Physik, Ludwig-Maximilians-Universität München, München, Germany
- ⁹⁹ Max-Planck-Institut für Physik (Werner-Heisenberg-Institut), München, Germany
- ¹⁰⁰ Nagasaki Institute of Applied Science, Nagasaki, Japan
- ¹⁰¹ Graduate School of Science, Nagoya University, Nagoya, Japan
- ¹⁰² ^(a) INFN Sezione di Napoli; ^(b) Dipartimento di Scienze Fisiche, Università di Napoli, Napoli, Italy
- ¹⁰³ Department of Physics and Astronomy, University of New Mexico, Albuquerque, NM, United States
- ¹⁰⁴ Institute for Mathematics, Astrophysics and Particle Physics, Radboud University Nijmegen/Nikhef, Nijmegen, Netherlands
- ¹⁰⁵ Nikhef National Institute for Subatomic Physics and University of Amsterdam, Amsterdam, Netherlands
- ¹⁰⁶ Department of Physics, Northern Illinois University, DeKalb, IL, United States
- ¹⁰⁷ Budker Institute of Nuclear Physics, SB RAS, Novosibirsk, Russia
- ¹⁰⁸ Department of Physics, New York University, New York, NY, United States
- ¹⁰⁹ Ohio State University, Columbus, OH, United States
- ¹¹⁰ Faculty of Science, Okayama University, Okayama, Japan
- ¹¹¹ Homer L. Dodge Department of Physics and Astronomy, University of Oklahoma, Norman, OK, United States
- ¹¹² Department of Physics, Oklahoma State University, Stillwater, OK, United States
- ¹¹³ Palacký University, RCPTM, Olomouc, Czech Republic
- ¹¹⁴ Center for High Energy Physics, University of Oregon, Eugene, OR, United States
- ¹¹⁵ LAL, Université Paris-Sud and CNRS/IN2P3, Orsay, France
- ¹¹⁶ Graduate School of Science, Osaka University, Osaka, Japan
- ¹¹⁷ Department of Physics, University of Oslo, Oslo, Norway
- ¹¹⁸ Department of Physics, Oxford University, Oxford, United Kingdom
- ¹¹⁹ ^(a) INFN Sezione di Pavia; ^(b) Dipartimento di Fisica, Università di Pavia, Pavia, Italy
- ¹²⁰ Department of Physics, University of Pennsylvania, Philadelphia, PA, United States
- ¹²¹ Petersburg Nuclear Physics Institute, Gatchina, Russia
- ¹²² ^(a) INFN Sezione di Pisa; ^(b) Dipartimento di Fisica E. Fermi, Università di Pisa, Pisa, Italy
- ¹²³ Department of Physics and Astronomy, University of Pittsburgh, Pittsburgh, PA, United States
- ¹²⁴ ^(a) Laboratório de Instrumentação e Física Experimental de Partículas – LIP, Lisboa, Portugal; ^(b) Departamento de Física Teórica y del Cosmos and CAFPE, Universidad de Granada, Granada, Spain
- ¹²⁵ Institute of Physics, Academy of Sciences of the Czech Republic, Praha, Czech Republic
- ¹²⁶ Faculty of Mathematics and Physics, Charles University in Prague, Praha, Czech Republic
- ¹²⁷ Czech Technical University in Prague, Praha, Czech Republic
- ¹²⁸ State Research Center Institute for High Energy Physics, Protvino, Russia
- ¹²⁹ Particle Physics Department, Rutherford Appleton Laboratory, Didcot, United Kingdom
- ¹³⁰ Physics Department, University of Regina, Regina, SK, Canada
- ¹³¹ Ritsumeikan University, Kusatsu, Shiga, Japan
- ¹³² ^(a) INFN Sezione di Roma I; ^(b) Dipartimento di Fisica, Università La Sapienza, Roma, Italy
- ¹³³ ^(a) INFN Sezione di Roma Tor Vergata; ^(b) Dipartimento di Fisica, Università di Roma Tor Vergata, Roma, Italy
- ¹³⁴ ^(a) INFN Sezione di Roma Tre; ^(b) Dipartimento di Fisica, Università Roma Tre, Roma, Italy
- ¹³⁵ ^(a) Faculté des Sciences Ain Chock, Réseau Universitaire de Physique des Hautes Energies – Université Hassan II, Casablanca; ^(b) Centre National de l’Energie des Sciences Techniques Nucleaires, Rabat; ^(c) Faculté des Sciences Semlalia, Université Cadi Ayyad, LPHEA-Marrakech; ^(d) Faculté des Sciences, Université Mohamed Premier and LPTPM, Oujda;
- ^(e) Faculté des Sciences, Université Mohammed V-Agdal, Rabat, Morocco
- ¹³⁶ DSM/IRFU (Institut de Recherches sur les Lois Fondamentales de l’Univers), CEA Saclay (Commissariat à l’Energie Atomique), Gif-sur-Yvette, France
- ¹³⁷ Santa Cruz Institute for Particle Physics, University of California Santa Cruz, Santa Cruz, CA, United States
- ¹³⁸ Department of Physics, University of Washington, Seattle, WA, United States
- ¹³⁹ Department of Physics and Astronomy, University of Sheffield, Sheffield, United Kingdom
- ¹⁴⁰ Department of Physics, Shinshu University, Nagano, Japan
- ¹⁴¹ Fachbereich Physik, Universität Siegen, Siegen, Germany
- ¹⁴² Department of Physics, Simon Fraser University, Burnaby, BC, Canada
- ¹⁴³ SLAC National Accelerator Laboratory, Stanford, CA, United States
- ¹⁴⁴ ^(a) Faculty of Mathematics, Physics & Informatics, Comenius University, Bratislava; ^(b) Department of Subnuclear Physics, Institute of Experimental Physics of the Slovak Academy of Sciences, Kosice, Slovak Republic
- ¹⁴⁵ ^(a) Department of Physics, University of Johannesburg, Johannesburg; ^(b) School of Physics, University of the Witwatersrand, Johannesburg, South Africa
- ¹⁴⁶ ^(a) Department of Physics, Stockholm University; ^(b) The Oskar Klein Centre, Stockholm, Sweden
- ¹⁴⁷ Physics Department, Royal Institute of Technology, Stockholm, Sweden
- ¹⁴⁸ Departments of Physics & Astronomy and Chemistry, Stony Brook University, Stony Brook, NY, United States
- ¹⁴⁹ Department of Physics and Astronomy, University of Sussex, Brighton, United Kingdom

- ¹⁵⁰ School of Physics, University of Sydney, Sydney, Australia
¹⁵¹ Institute of Physics, Academia Sinica, Taipei, Taiwan
¹⁵² Department of Physics, Technion: Israel Institute of Technology, Haifa, Israel
¹⁵³ Raymond and Beverly Sackler School of Physics and Astronomy, Tel Aviv University, Tel Aviv, Israel
¹⁵⁴ Department of Physics, Aristotle University of Thessaloniki, Thessaloniki, Greece
¹⁵⁵ International Center for Elementary Particle Physics and Department of Physics, The University of Tokyo, Tokyo, Japan
¹⁵⁶ Graduate School of Science and Technology, Tokyo Metropolitan University, Tokyo, Japan
¹⁵⁷ Department of Physics, Tokyo Institute of Technology, Tokyo, Japan
¹⁵⁸ Department of Physics, University of Toronto, Toronto, ON, Canada
¹⁵⁹ ^(a) TRIUMF, Vancouver BC; ^(b) Department of Physics and Astronomy, York University, Toronto, ON, Canada
¹⁶⁰ Institute of Pure and Applied Sciences, University of Tsukuba, 1-1-1 Tennodai, Tsukuba, Ibaraki 305-8571, Japan
¹⁶¹ Science and Technology Center, Tufts University, Medford, MA, United States
¹⁶² Centro de Investigaciones, Universidad Antonio Narino, Bogota, Colombia
¹⁶³ Department of Physics and Astronomy, University of California Irvine, Irvine, CA, United States
¹⁶⁴ ^(a) INFN Gruppo Collegato di Udine; ^(b) ICTP, Trieste; ^(c) Dipartimento di Chimica, Fisica e Ambiente, Università di Udine, Udine, Italy
¹⁶⁵ Department of Physics, University of Illinois, Urbana, IL, United States
¹⁶⁶ Department of Physics and Astronomy, University of Uppsala, Uppsala, Sweden
¹⁶⁷ Instituto de Física Corpuscular (IFIC) and Departamento de Física Atómica, Molecular y Nuclear and Departamento de Ingeniería Electrónica and Instituto de Microelectrónica de Barcelona (IMB-CNM), University of Valencia and CSIC, Valencia, Spain
¹⁶⁸ Department of Physics, University of British Columbia, Vancouver, BC, Canada
¹⁶⁹ Department of Physics and Astronomy, University of Victoria, Victoria, BC, Canada
¹⁷⁰ Department of Physics, University of Warwick, Coventry, United Kingdom
¹⁷¹ Waseda University, Tokyo, Japan
¹⁷² Department of Particle Physics, The Weizmann Institute of Science, Rehovot, Israel
¹⁷³ Department of Physics, University of Wisconsin, Madison, WI, United States
¹⁷⁴ Fakultät für Physik und Astronomie, Julius-Maximilians-Universität, Würzburg, Germany
¹⁷⁵ Fachbereich C Physik, Bergische Universität Wuppertal, Wuppertal, Germany
¹⁷⁶ Department of Physics, Yale University, New Haven, CT, United States
¹⁷⁷ Yerevan Physics Institute, Yerevan, Armenia
¹⁷⁸ Domaine scientifique de la Doua, Centre de Calcul CNRS/IN2P3, Villeurbanne Cedex, France

^a Also at Laboratório de Instrumentação e Física Experimental de Partículas – LIP, Lisboa, Portugal.

^b Also at Faculdade de Ciências and CFNUL, Universidade de Lisboa, Lisboa, Portugal.

^c Also at Particle Physics Department, Rutherford Appleton Laboratory, Didcot, United Kingdom.

^d Also at TRIUMF, Vancouver, BC, Canada.

^e Also at Department of Physics, California State University, Fresno, CA, United States.

^f Also at Novosibirsk State University, Novosibirsk, Russia.

^g Also at Fermilab, Batavia, IL, United States.

^h Also at Department of Physics, University of Coimbra, Coimbra, Portugal.

ⁱ Also at Department of Physics, UASLP, San Luis Potosi, Mexico.

^j Also at Università di Napoli Parthenope, Napoli, Italy.

^k Also at Institute of Particle Physics (IPP), Canada.

^l Also at Department of Physics, Middle East Technical University, Ankara, Turkey.

^m Also at Louisiana Tech University, Ruston, LA, United States.

ⁿ Also at Dep. Física and CEFITEC of Faculdade de Ciências e Tecnologia, Universidade Nova de Lisboa, Caparica, Portugal.

^o Also at Department of Physics and Astronomy, University College London, London, United Kingdom.

^p Also at Group of Particle Physics, University of Montreal, Montreal, QC, Canada.

^q Also at Department of Physics, University of Cape Town, Cape Town, South Africa.

^r Also at Institute of Physics, Azerbaijan Academy of Sciences, Baku, Azerbaijan.

^s Also at Institut für Experimentalphysik, Universität Hamburg, Hamburg, Germany.

^t Also at Manhattan College, New York, NY, United States.

^u Also at School of Physics, Shandong University, Shandong, China.

^v Also at CPPM, Aix-Marseille Université and CNRS/IN2P3, Marseille, France.

^w Also at School of Physics and Engineering, Sun Yat-sen University, Guanzhou, China.

^x Also at Academia Sinica Grid Computing, Institute of Physics, Academia Sinica, Taipei, Taiwan.

^y Also at Dipartimento di Fisica, Università La Sapienza, Roma, Italy.

^z Also at DSM/IRFU (Institut de Recherches sur les Lois Fondamentales de l'Univers), CEA Saclay (Commissariat à l'Energie Atomique), Gif-sur-Yvette, France.

^{aa} Also at Section de Physique, Université de Genève, Geneva, Switzerland.

^{ab} Also at Departamento de Física, Universidade de Minho, Braga, Portugal.

^{ac} Also at Department of Physics and Astronomy, University of South Carolina, Columbia, SC, United States.

^{ad} Also at Institute for Particle and Nuclear Physics, Wigner Research Centre for Physics, Budapest, Hungary.

^{ae} Also at California Institute of Technology, Pasadena, CA, United States.

^{af} Also at Institute of Physics, Jagiellonian University, Krakow, Poland.

^{ag} Also at LAL, Université Paris-Sud and CNRS/IN2P3, Orsay, France.

^{ah} Also at Department of Physics and Astronomy, University of Sheffield, Sheffield, United Kingdom.

^{ai} Also at Department of Physics, Oxford University, Oxford, United Kingdom.

^{aj} Also at Institute of Physics, Academia Sinica, Taipei, Taiwan.

^{ak} Also at Department of Physics, The University of Michigan, Ann Arbor, MI, United States.

* Deceased.